WILEY | Hindawi

Research Article

Numerical Simulation and Sensitivity Analysis of Hydraulic Fracturing in Multilayered Thin Tight Sandstone Gas Reservoir

Hao Zhang [ID], Yuhu Bai, Bingxiang Xu, Xulin Du, and Shaohua Gai

CNOOC Research Institute Co., Ltd., Beijing 100028, China

Correspondence should be addressed to Hao Zhang; zhanghao82@cnooc.com.cn

Hydraulic fracturing is a necessary measurement to realize the commercial exploitation of oil and gas, but its application in multilayered thin tight sandstone gas reservoirs is still not perfect, which usually have thin gas layers mixed with complex intervals, and shows a dramatic variation in geological and geomechanical properties in the vertical direction. When conventional hydraulic fracturing methods are applied to this kind of reservoir, it is hard to get proper fracture propagation, especially for fracture height control. Facing this situation, this paper proposes a numerical study of the hydraulic fracturing mechanism and analyzes its influencing factors in the multilayered thin tight sandstone gas reservoir. Relying on a real reservoir in the Ordos Basin in China, relevant geological and geomechanical parameters of major gas layers and interlayers are obtained. According to these parameters, the hydraulic fracturing simulation in the multilayered thin tight gas reservoir model is carried out, based on which, the sensitivity analysis of different geological and fracturing parameters which affect the fracture propagation is performed. Furthermore, a real low-production well after fracturing in this kind of reservoir is selected as an example, and based on the analysis, an optimized fracturing scheme is proposed to adapt to the characteristics of the reservoir. According to the comparison of fracturing and production simulations, the optimized fracturing scheme can prevent hydraulic fractures from breaking through thin interlayers, control the fracture height, and prevent fractures from communicating strata with a high water-bearing layer. At the same time, with the same amount of proppant and fracturing fluid, longer fracture length and better fracture conductivity are created, so that the productivity of the optimized fracture has been greatly improved.

1. Introduction

As an unconventional hydrocarbon resource, tight sandstone gas is widely distributed and has abundant reserves. The proven recoverable tight gas is nearly 40% of the total proven reserves of natural gas, which shows huge development potential [1]. However, the tight gas reservoir has the characteristics of low porosity and permeability, insufficient natural energy, and poor fluidity, which make it difficult to form commercial exploitation by conventional methods [2], while hydraulic fracturing is an effective method for commercial exploitation of tight gas [3].

The numerical simulation method can conveniently and efficiently study the propagation mechanism and influencing factors of hydraulic fractures in the formation, so as to formulate more reasonable fracturing and development strategies. Scholars have researched the simulation study of hydraulic fracture propagation for decades. Some models developed in the early decades laid the foundation for the simulation of hydraulic fracturing. The most representative ones are the KGD model [4] and the PKN model [5], for which the KGD model is more suitable for the case when fracture length is not much longer than the fracture height, while the PKN model is more suitable for the case when the fracture length is much longer than the fracture height [6]. On this basis, many numerical models for hydraulic fracture propagation have been gradually developed and can be summarized into three categories: boundary element model (BEM) [7], finite element model (FEM) [8], and discrete element model (DEM) [9]. Comparing the FEM and DEM, the BEM only needs to divide the simulated fracture surface, not the entire domain, which gives it a fast simulation speed and
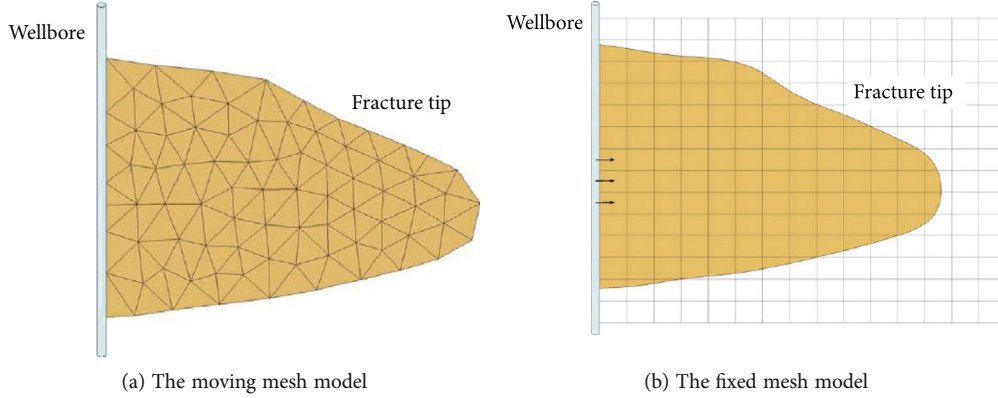
(a) The moving mesh model

(b) The fixed mesh model

FIGURE 1: Two kinds of PL3D model system [17].

strong flexibility. Scholars have used the BEM to construct the numerical model of multibranched fractures, which can realize the propagation simulation of complex fracture networks [10, 11]. Recently, with the concept of stimulation reservoir volume (SRV) [12], volume fracturing has also become a research hotspot in the field of hydraulic fracturing, and more complex fracture network propagation models have also been proposed and improved [13, 14].

The traditional two-dimensional hydraulic fracture propagation models are suitable to simulate the lateral propagation of hydraulic fractures in the horizontal direction of the reservoir. However, the actual reservoirs usually have complex strata structures, and the vertical propagation of hydraulic fractures is also worth studying. Therefore, based on the two-dimensional model, scholars have developed pseudo-three-dimensional (P3D) and full three-dimensional models of hydraulic fractures. The pseudo-three-dimensional model introduces the fracture height into the two-dimensional fracture propagation criterion and calculates the fracture height by judging the fracture's propagation, and the fluid in fracture only considers one-dimensional flow [15]; while the full three-dimensional model considers three-dimensional rock deformation and two-dimensional fluid flow to simulate the fracture propagation process more precisely, which inevitably makes simulation very difficult [16]. In recent years, based on the PKN model, the planar three-dimensional (PL3D) model has been proposed and applied by several kinds of commercial hydraulic fracturing simulators and shows good simulation performance for multilayered fracturing [17].

At present, the application of hydraulic fracturing in tight gas development is still far from perfect. The tight gas reservoirs in China are usually with small areas and complex vertical strata, and the gas layers are thin and usually interspersed with water-bearing layers and fragile interlayers, which makes hydraulic fractures easily breakthrough the interlayer and enter the water-bearing layer, resulting in a low production of gas wells. Therefore, the hydraulic fracturing methods developed based on shale oil and gas reservoirs with large areas and thicknesses which cannot be directly used in the development of multilayered thin tight gas reservoirs, and it is necessary to develop a suitable

TABLE 1: The type of different formation layers in the tight gas reservoir.

| Layer types	Descriptions
Layer type 1	The tight sandstone layer in the Shanxi formation
Layer type 2	The mudstone layer in the Shanxi formation
Layer type 3	The mudstone and coal seam overlapping layer between Shanxi and Taiyuan formation
Layer type 4	The tight sandstone layer in the Taiyuan formation
Layer type 5	The thick coal seam between Taiyuan and Benxi formation
Layer type 6	The mudstone and coal seam overlapping layer in the Benxi formation
Layer type 7	The tight sandstone layer in the Benxi formation
Layer type 8	The marl bedrock in the Benxi formation

hydraulic fracturing method. Based on the above situation, this paper relies on a real tight gas reservoir in the Ordos Basin to study the hydraulic fracture propagation in multilayered thin tight gas reservoirs. Firstly, the numerical simulation method of hydraulic fracture propagation is described. Secondly, the logging parameters of some real wells are counted, including the geological and geomechanical data of major gas layers and interlayers; then, a hydraulic fracturing model is constructed accordingly by using the StimPlan software. Thirdly, based on the numerical model, the impact of different geological and fracturing parameters on the shape of hydraulic fractures is analyzed. Finally, a low-production well after fracturing in this reservoir is selected as an example, the reasons for the low production is analyzed according to the fracturing simulation results, and an optimized fracturing scheme is proposed to generate a better hydraulic fracture which is more adaptive to the characters of this multilayered thin tight gas reservoir.

2. The Numerical Model of Hydraulic Fracture Propagation in Multilayered Reservoirs and the Influencing Factors
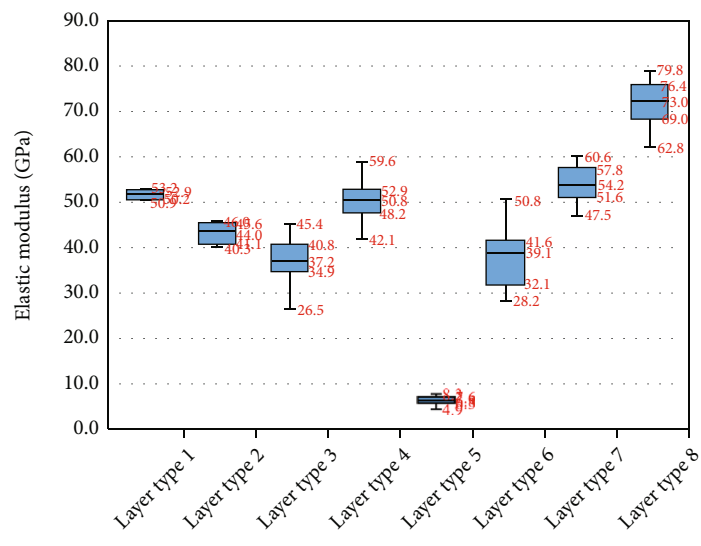
As can be seen from the introduction section, there are several kinds of hydraulic fracturing numerical models. In this
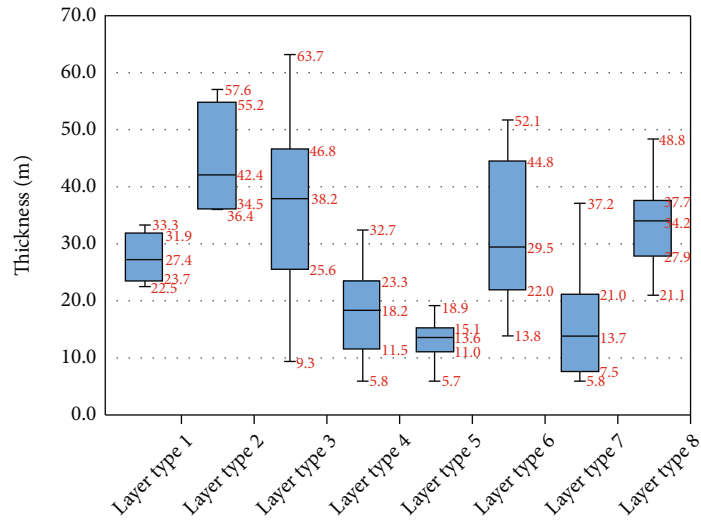
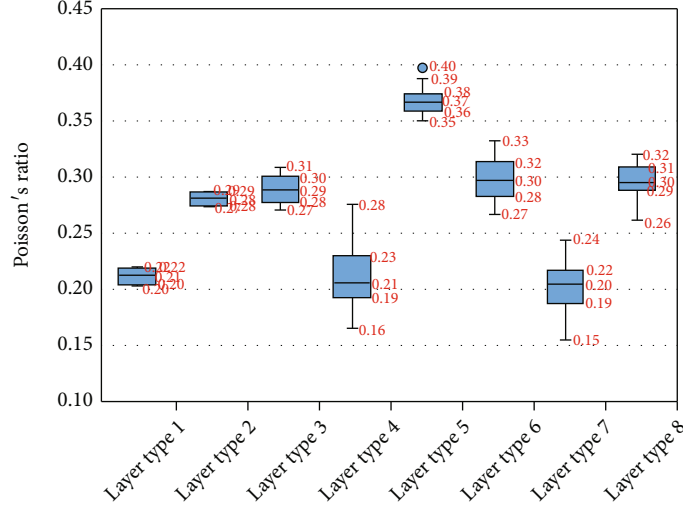(a) The distribution of thickness
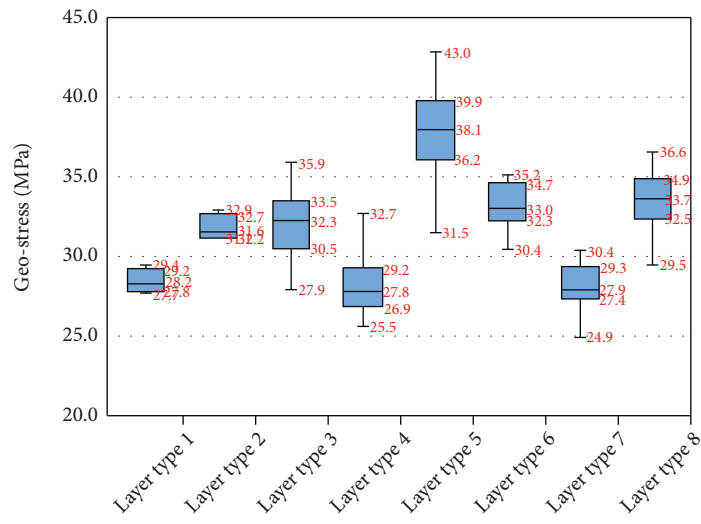
(b) The distribution of geostress

(c) The distribution of elastic modulus

Figure 2: Continued.

(d) The distribution of Poisson's ratio

FIGURE 2: The distribution of the geological data of different layer types.

TABLE 2: The mean value and variation range of the geological parameters in different layer types.

	Thickness (m)			Poisson's ratio			Elastic modulus (GPa)			Geostress (MPa)		
	Mean	Max	Min	Mean	Max	Min	Mean	Max	Min	Mean	Max	Min
Layer type 1	27.6	33.3	22.5	0.21	0.22	0.2	52.05	53.18	50.88	28.34	29.44	27.68
Layer type 2	44.7	57.6	36.4	0.28	0.29	0.27	43.89	46.05	40.25	31.92	32.93	31.2
Layer type 3	38	63.7	9.3	0.29	0.31	0.27	38.56	45.39	26.54	32.26	35.92	27.92
Layer type 4	19.2	46.1	5.8	0.22	0.28	0.16	49.59	59.57	42.14	27.89	32.7	25.55
Layer type 5	13	18.9	5.7	0.37	0.41	0.35	6.92	9.69	4.91	37.57	42.96	31.55
Layer type 6	31.6	52.1	13.8	0.3	0.33	0.27	38.3	50.8	28.23	33.29	35.19	30.42
Layer type 7	15.2	37.2	5.8	0.2	0.24	0.15	53.68	60.61	47.5	28.19	30.37	24.91
Layer type 8	33.3	48.8	21.1	0.3	0.32	0.26	71.45	79.8	47.09	33.74	36.61	29.5

paper, the multilayered hydraulic fracturing model is constructed by using the StimPlan software, which is a powerful commercial hydraulic fracturing numerical simulation software that ensembles various fracture propagation models including the P3D [18] and PL3D models and can realize the precise 3D hydraulic fracturing in the multilayered reservoir. Based on this software, the numerical model for PL3D hydraulic fracturing simulation is illustrated.

2.1. The Mathematical Functions of the PL3D Model. The PL3D model is derived from the assumption of the PKN model, and during numerical simulation, the fracture is subdivided into several FraC-meshes, which can be classified into the moving mesh system and the fixed mesh system, respectively (Figure 1) [17]. In 1979, Clifton and Abou-Sayed [16] proposed the moving mesh-based PL3D model, and then in 2002, Siebrits and Peirce [19] presented the fixed mesh-based PL3D model.

The governing functions for the PL3D model consist of: (I) elastic function that relates fluid pressure on the fracture opening; (II) fluid flow function that relates fluid flow in the fracture on the fracture opening; (III) fracture criterion that relates the fracture propagation state on the fracture opening. These functions are introduced briefly as follows.

During the fracture propagation in the 3D space, the fracture width is related to the 2D-distributed fluid pressure with a single integral based on the elasticity theory, so the elastic function can be written as follows:

$$p - \sigma_0 = \frac{G}{4\pi(1-v)} \iint \left(\frac{\partial}{\partial y'} \left(\frac{1}{R} \right) \frac{\partial w}{\partial y'} + \frac{\partial}{\partial x'} \left(\frac{1}{R} \right) \frac{\partial w}{\partial x'} \right) dx' dy',$$

(1)

where p is the fluid pressure acting on the fracture surface, σ_0 is the minimum horizontal stress, G is the shear modulus, and v is the Poisson's ratio. w is the fracture width at the points (x', y'); R presents the distance between the points (x, y) at which the pressure is applied and the point (x', y') at which the integrand is being evaluated and can be written as follows:

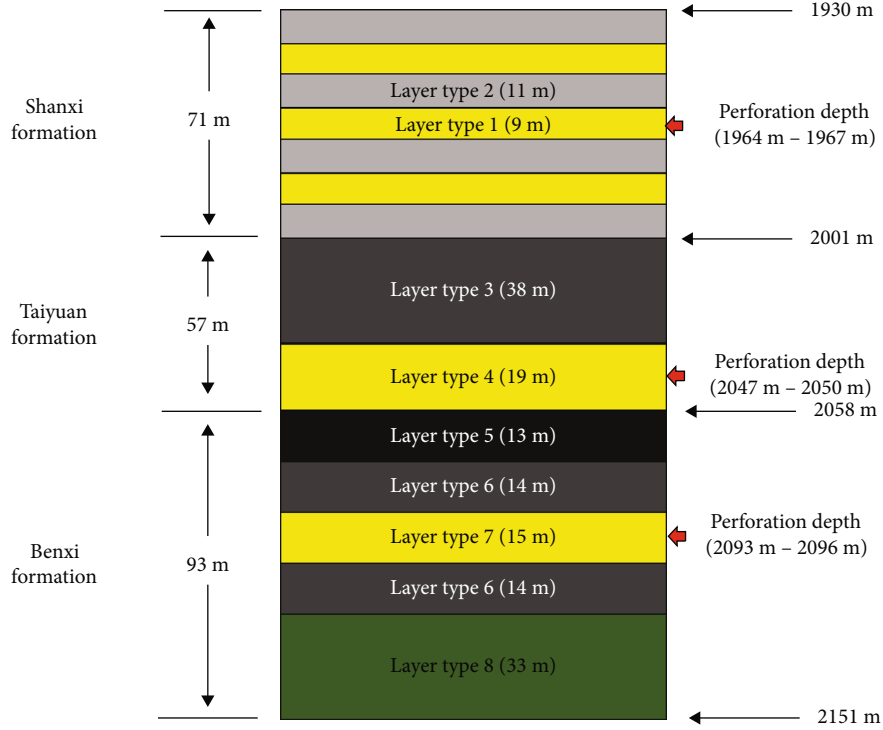$$R = \sqrt{\left(x - x' \right)^2 + \left(y - y' \right)^2}.$$

(2)

FIGURE 3: The concept model of the multilayered thin tight gas reservoir.
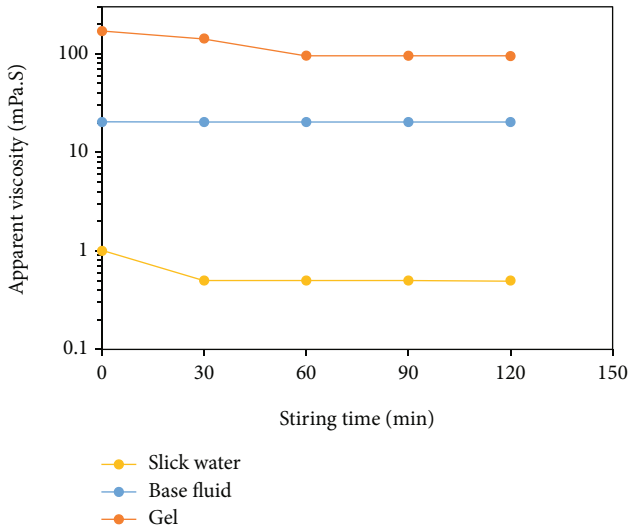
FIGURE 4: Rheological parameters of different fracturing fluids.

where q is the flow rate, and q_x and q_y are the divert flow rates along the x and y directions; n and k are the rheological parameters related to the fracturing fluid, ρ_f is the density of fracturing fluid, and g_y is the gravitational acceleration along the y direction.

The fluid flow function should be calculated considering the fluid continuity. The fluid continuity function of the PL3D model is similar to the P3D model, but the fluid flow in the y direction is also considered

$$\frac{\partial q_x}{\partial x} + \frac{\partial q_y}{\partial y} + q_L = -\frac{\partial w}{\partial t}, \tag{5}$$

where q_L represents the leakoff fluid, and according to Carter's leakoff model, the q_L can be written as follows:

$$q_L = \frac{2C_l}{\sqrt{t - \tau(x, y)}}, \tag{6}$$

where t is the total fracturing time; $\tau(x)$ is the time when the fracture first reaches the position (x, y); C_l is Carter's leakoff coefficient, which is related to the factors like formation permeability and fluid viscosity.

The LEFM theory [20] is adopted as the propagation criterion along the fracture edges. According to this theory, the model I stress intensity factor (K_I) is used to calculate the critical fracture width

$$w_{\text{crit}} = \frac{4K_I(1 - \nu)}{G}\left(\frac{a}{2\pi}\right)^{1/2}, \tag{7}$$

The elastic function is calculated along with the fluid flow function, different from the 1D flow in the P3D model, and the 2D flow is considered in the PL3D model. Based on Poiseuille's law, the fluid flow in the fracture is

$$\frac{\partial p}{\partial x} + \left[k\left(2 + \frac{1}{n}\right)\frac{2(n + 1)}{n}\right]^{1/n}\left(\frac{|q|}{w^2}\right)^{n-1}\frac{q_x}{w^3} = 0, \tag{3}$$

$$\frac{\partial p}{\partial y} + \left[k\left(2 + \frac{1}{n}\right)\frac{2(n + 1)}{n}\right]^{1/n}\left(\frac{|q|}{w^2}\right)^{n-1}\frac{q_y}{w^3} = \rho_f g_y, \tag{4}$$

TABLE 3: The injection procedure for hydraulic fracturing simulation.

Fracturing injection stage	Injection volume (m^3)	Proppant concentration (kg/m^3)	Injection rate (m^3/min)	Single-stage injection time (min)	Total injection time (min)	Fluid type	Proppant type
1	40	0	3.5	11.4	11.4	Base fluid	/
2	19.96	73	3.5	5.8	17.3	Base fluid	40/70 mesh
3	35	0	3.5	10.0	27.3	Base fluid	/
4	15.04	102	3.5	4.5	31.7	Gel	30/50 mesh
5	22.99	203	3.5	7.0	38.7	Gel	30/50 mesh
6	30.02	290	3.5	9.5	48.2	Gel	30/50 mesh
7	45.02	363	3.5	14.6	62.8	Gel	30/50 mesh
8	35.03	435	3.5	11.6	74.4	Gel	30/50 mesh
9	19.99	508	3.5	6.8	81.1	Gel	30/50 mesh
10	6.6	0	3.5	1.9	83.0	Gel	30/50 mesh

where w_{crit} is the critical fracture width; a is a small distance close to the fracture edge. Usually, the model I stress intensity factor (K_I) equals the rock toughness.

To simulate the fracture propagation, first, discretize the plane for fracture propagation into discrete elements and set the initial fracture element, the initial fluid pressure p, and the simulation time step Δt; then calculate the fluid flow function in Equations (3)–(4) by coupling the fluid continuity function in Equation (5) based on the given geological parameters to obtain the fracture width w; third, calculate the elastic function in Equation (1) using the calculated w to obtain the new fluid pressure p. Compare the new fluid pressure with the initial fluid pressure, if not converge, set the new fluid pressure as the initial fluid pressure and restart the iteration, until these two fluid pressure converge. Once one simulation time step is done and the width of fracture edge elements is obtained, it will be evaluated by the critical fracture width in Equation (7), and if the width of the fracture edge is larger than the critical fracture width, the fracture will continue propagating, then add elements opened by the fracture edge into the fracture and back to the iteration procedure to recalculate the fluid pressure and width for the new fracture. Repeat this procedure and continue increasing the fracture elements until the fracturing injection operation is completed. Then, the fracture half-length and height can be obtained by summing up all the elements opened by the fracture, and the fracture width is obtained by the last simulation time step.

Based on the mathematical functions of the PL3D model, the StimPlan software rigorously solves the propagation of hydraulic fractures and obtains more accurate 2D planar fracture geometry in 3D multilayered formations, and the more detailed illustration of the PL3D fracture model in the StimPlan can be found in these articles [19, 21, 22].

2.2. The Major Influencing Factor for Hydraulic Fracture Propagation in Multilayered Reservoirs. The hydraulic fracture propagation in the multilayered reservoir is affected by various factors, which can be mainly divided into two categories: the first category is the reservoir geological parameters like in situ stress, elastic modulus, Poisson's ratio, and reservoir layer thickness; the second category is the fractur-
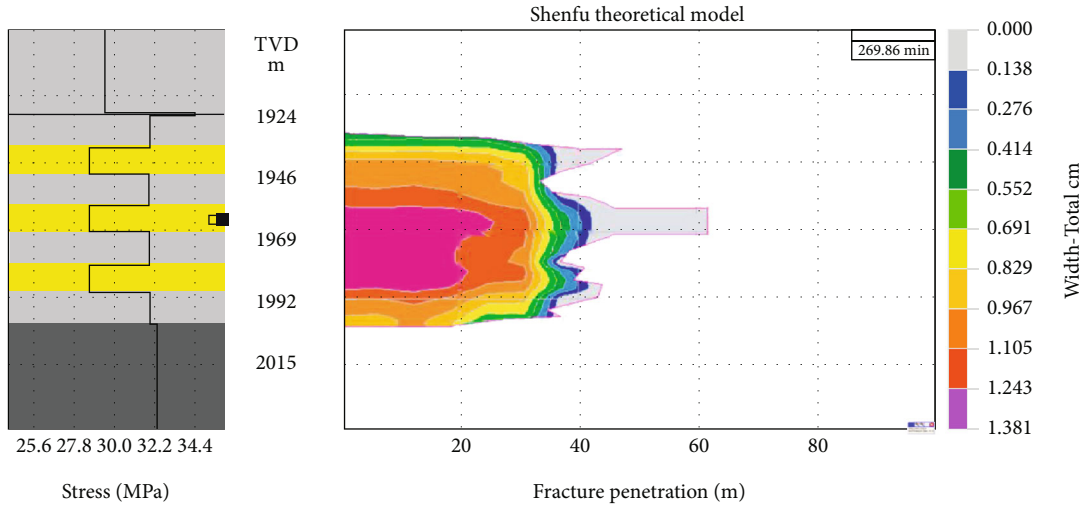
ing operational parameters including fracturing fluid viscosity, fracturing fluid injection rate, and total fracturing fluid injection volume. Besides, for hydraulic fracturing involving proppant, the influence of proppant concentration should also be considered.

3. The Construction of the Multilayered Thin Tight Sandstone Gas Reservoir Model and the Hydraulic Fracturing Simulation

In this paper, we construct a multilayered thin tight sandstone gas reservoir model based on a real reservoir located in the Ordos Basin in China. The types of this gas reservoir are mainly low production, ultralow abundance, and medium-shallow tight sandstone gas reservoirs.

3.1. The Statistics of Geological and Parameters. There are several sets of reservoir-caprock assemblages developed in the strata of this reservoir, forming multiple overlapping sets of gas layers and interlayers. The formations in this reservoir can be divided into the Shanxi formation, Taiyuan formation, and Benxi formation from top to bottom. The Shanxi formation is mainly composed of overlapping tight sandstone and mudstone intervals, interspersed with some thin coal seams. There are many thin coal seams and mudstone overlapping intervals between the Taiyuan formation and Shanxi formation. There are also several overlapping coal seams and mudstone layers between the Taiyuan formation and Benxi formation, including a thick coal seam with a thickness of more than 10 meters. Below the Benxi formation is the bedrock composed of marl. The formation layers in the tight gas reservoir are summarized into several types as shown in Table 1.

The relative geological parameters of the above formation layers are counted from the well-logging data of tens of real wells in this tight gas reservoir, which includes layer thickness, in situ stress, elastic modulus, and Poisson's ratio. The distribution of these parameters can be seen in Figure 2, and the variation range and the mean value of these parameters in each layer are shown in Table 2.

(a) The hydraulic fracture in Shanxi formation

(b) The hydraulic fracture in Taiyuan formation

Figure 5: Continued.
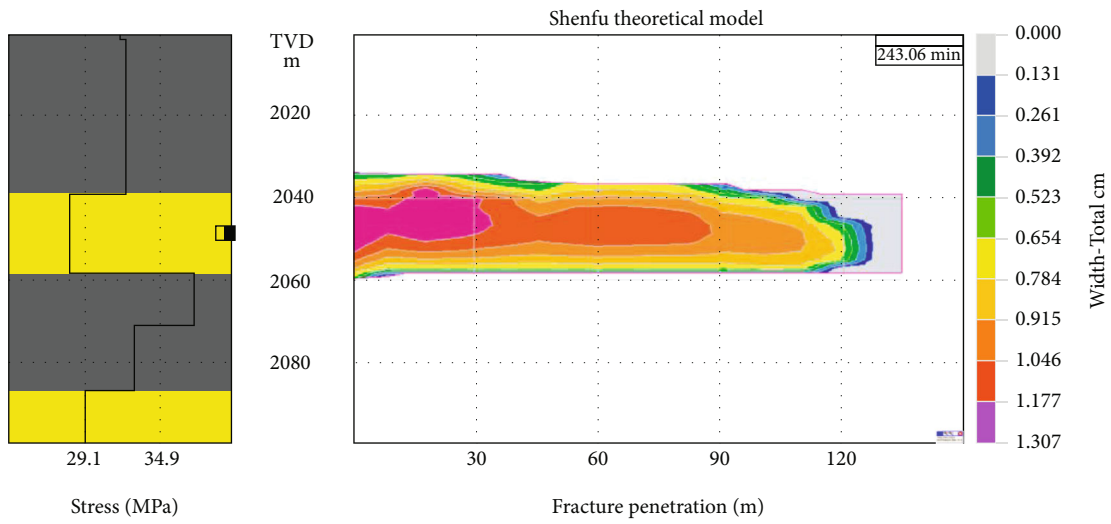
Lithologies:

- ■ Coal (black)
- ■ Sandstone (yellow)
- ■ Mudstone & Coal overlapping (gray)
- ■ Marl (green)
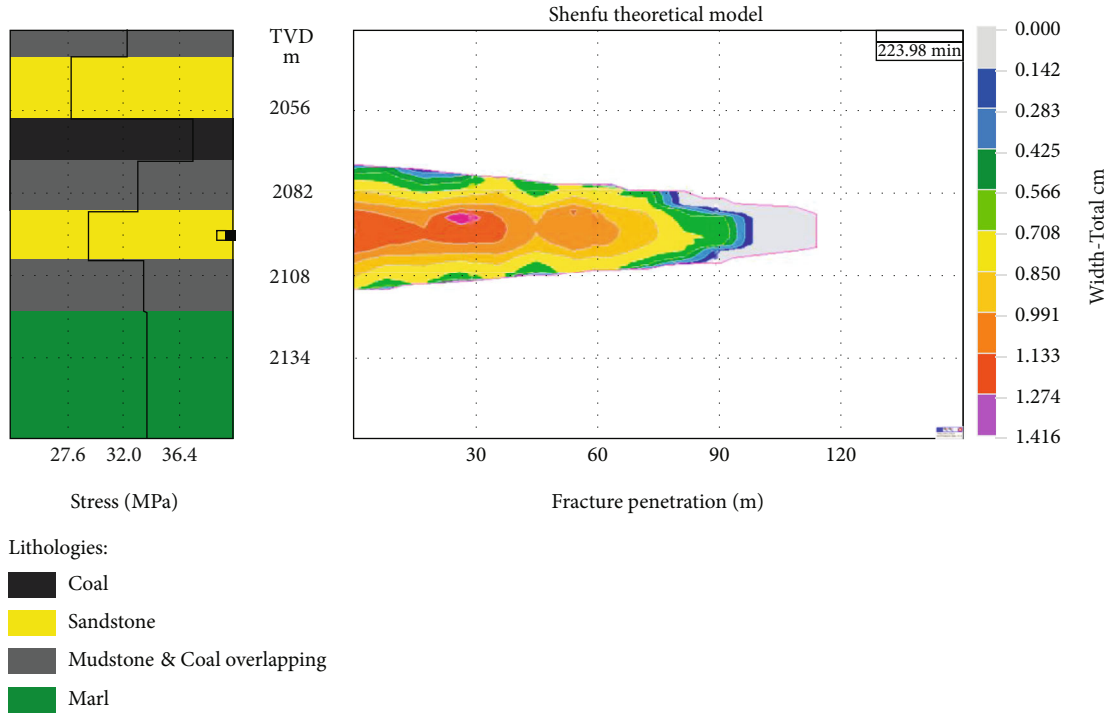
(c) The hydraulic fracture in Benxi formation

- ■ Shanxi formation
- ■ Taiyuan formation
- ■ Benxi formation
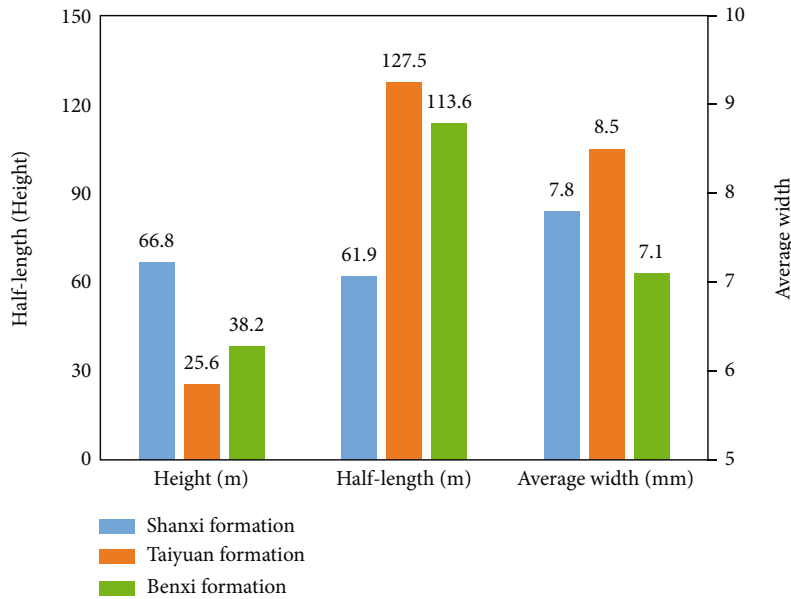
(d) The statistic of the hydraulic fracture parameters for each formation

FIGURE 5: The numerical hydraulic fracture models after simulation.

3.2. The Construction of the Multilayered Thin Tight Sandstone Gas Reservoir.

According to the statistical results of each layer, a numerical model for this multilayered thin tight gas reservoir is constructed by using the StimPlan software [17]. As shown in Figure 3, the numerical reservoir model is a conceptual model which is constructed by the mean value of each type of layer in Table 2 and aims to reflect the main character of this multilayered thin tight reservoir.

This reservoir conceptual model fully reflects the actual stratigraphic distribution of this multilayered thin tight gas reservoir. A three-layer sandstone-mudstone overlapping interval is constructed to represent the geological structure of the Shanxi formation; the formation between sandstones of the Shanxi and Taiyuan formations is a thick mudstone-coal interval; the sandstone of the Benxi formation is surrounded by upper and lower layers of mudstone-coal
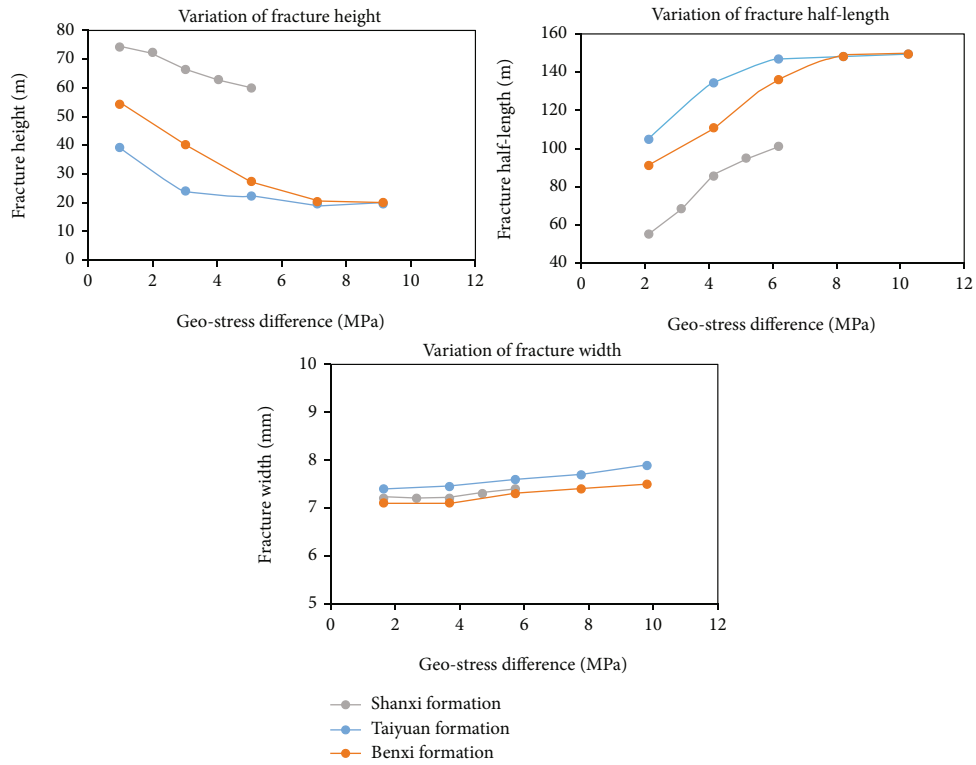
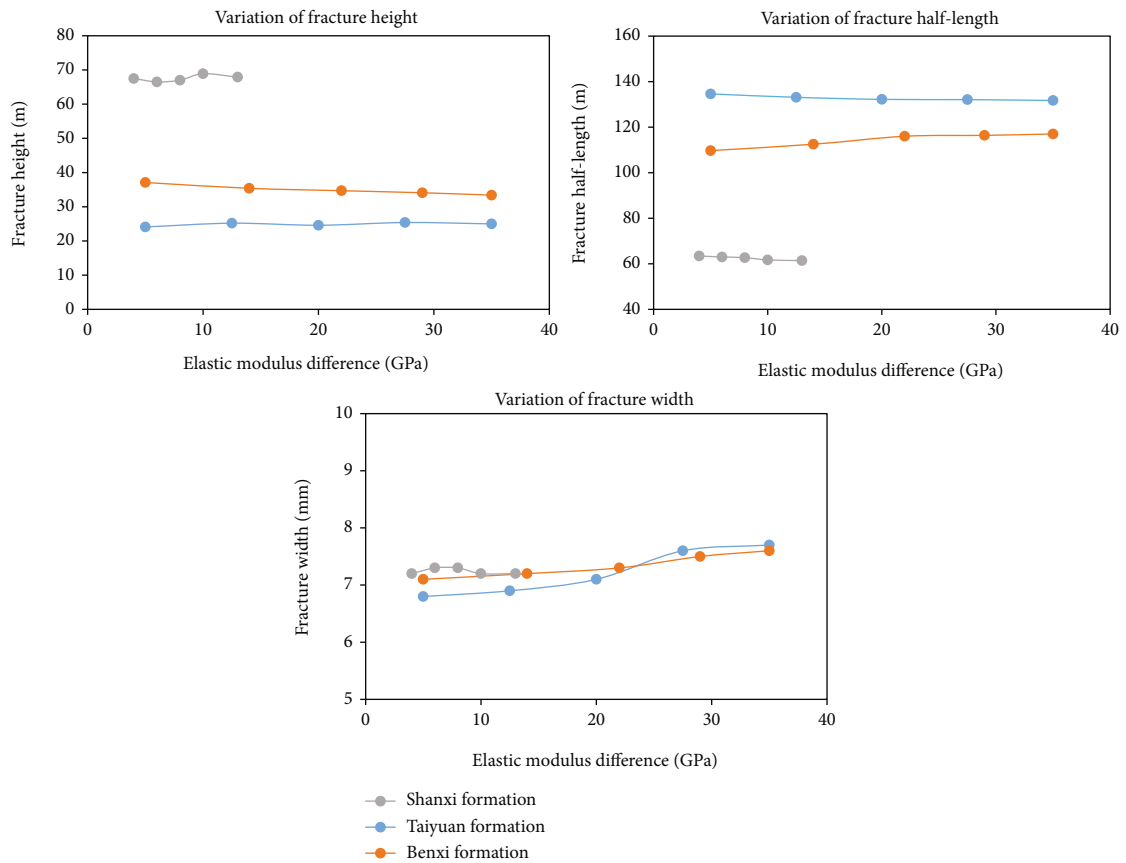Figure 6: Variation of hydraulic fracture shape with the geostress difference.

Figure 7: Variation of hydraulic fracture shape with the elastic modulus difference.
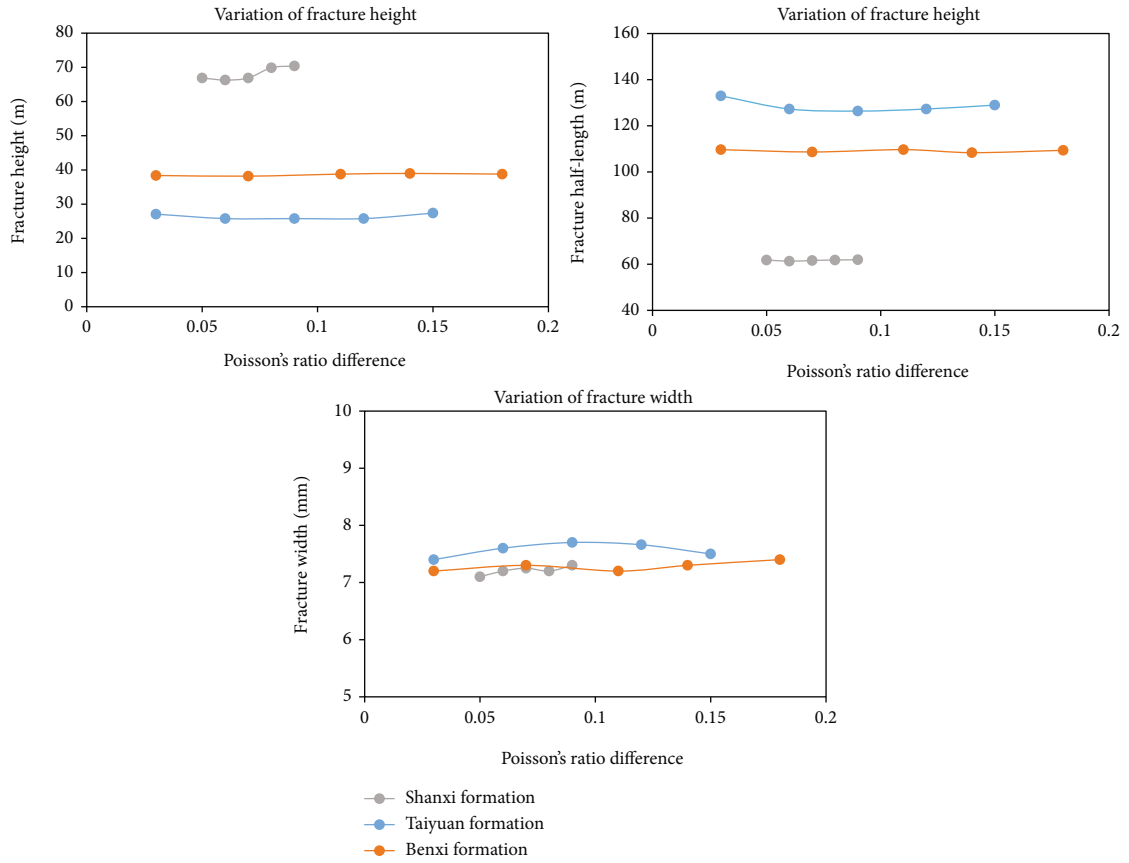
Figure 8: Variation of hydraulic fracture shape with the Poisson's ratio difference.
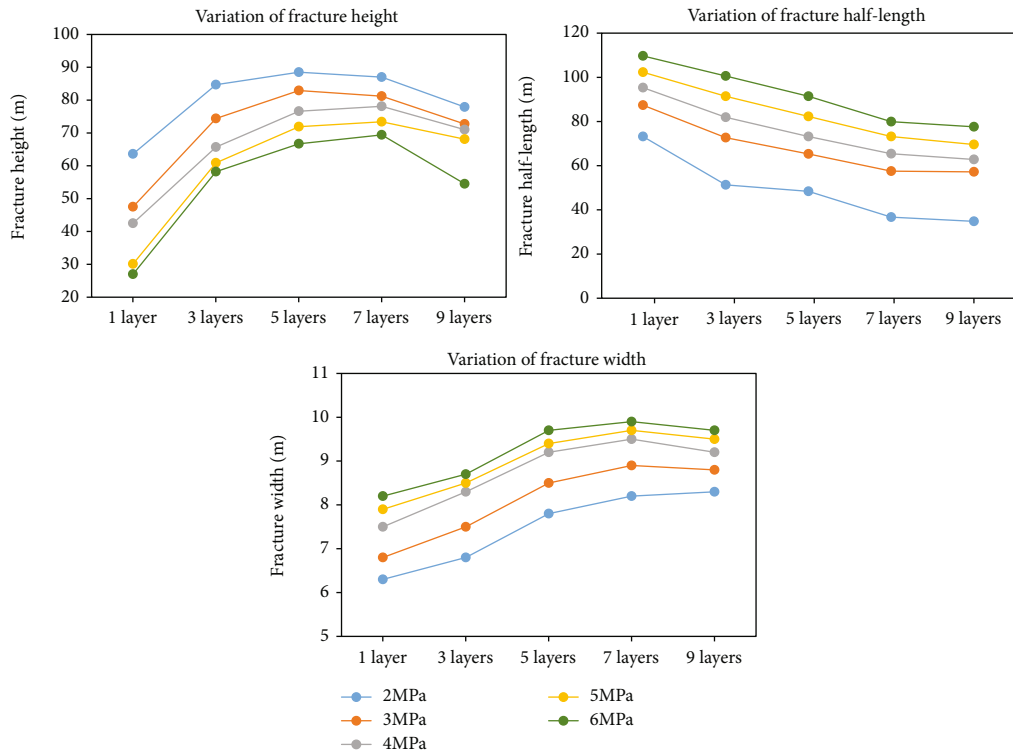

Figure 9: Variation of hydraulic fracture shape with the geostress and layer number.
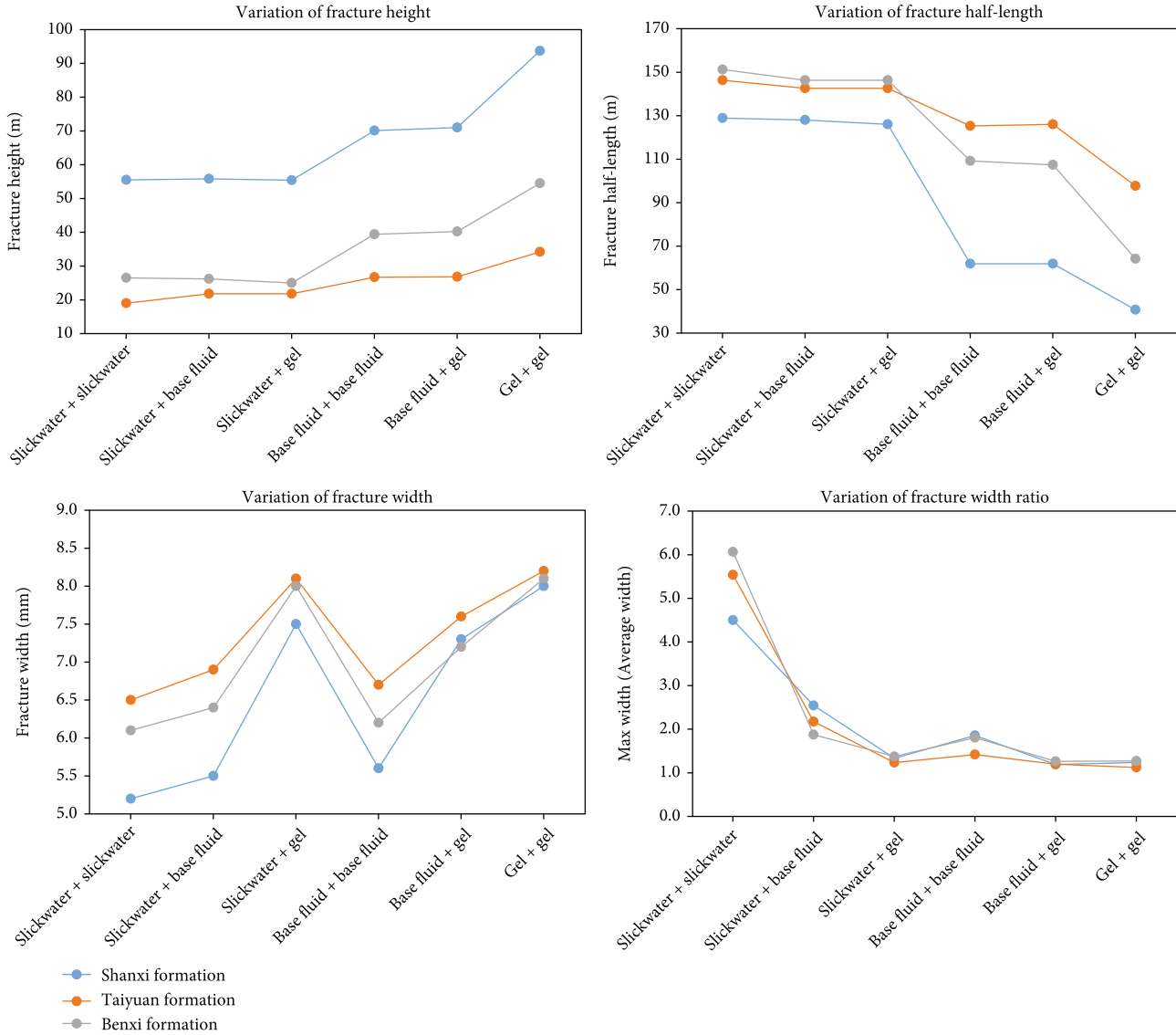
FIGURE 10: Variation of hydraulic fracture shape with the fracturing fluid viscosity.

interval. Between the Shanxi and Benxi formation is a thick coal seam, and the formation below the Benxi is a marl bedrock.

3.3. The Hydraulic Fracturing Numerical Simulation in the Multilayered Thin Tight Sandstone Gas Reservoir. According to the actual hydraulic fracturing operation, the fracturing fluid used in this reservoir is a CPF-WBFF-FW fracturing fluid system, consisting of a low-viscosity fracturing base fluid (base fluid for short) and a high-viscosity gel, and the proppant used is 40/70 mesh and 30/50 mesh ceramic proppant. To make a comparison, slickwater is introduced as the additional fracturing fluid in this study, and the relevant rheological parameters are shown in Figure 4. According to the actual hydraulic fracturing operation in this reservoir, the fracturing pump injection procedure of this model is shown in Table 3.

The well used in the model is set as a vertical well with a depth of 2150 m, penetrating the three formations. The ID of

the casing in the well is 139.7 mm, and the perforation is performed at the middle depth of the sandstone layer for these three formation groups. The length of the perforation section is 3 m, the perforation density is 16 holes/m, and the hole diameter is 10.6 mm. According to the above model and parameters, the hydraulic fracturing in the three formations is simulated based on the pump injection procedure in Table 3, respectively, and the fractures in these three formations are shown in Figure 5.

It can be seen from the above results that under the same pump injection procedure, the hydraulic fracture in the Shanxi formation has the shortest half-length and the highest height. It is because the interlayer between the sandstone in Shanxi formation consists of mudstone, and the statistical result in Figure 2 shows that the geomechanical properties of mudstone are similar to that of the sandstone. Besides, the mudstone interlayer is thin, and the geostress difference between the sandstone and mudstone interlayer is small. All of these reasons make the hydraulic fracture can easily
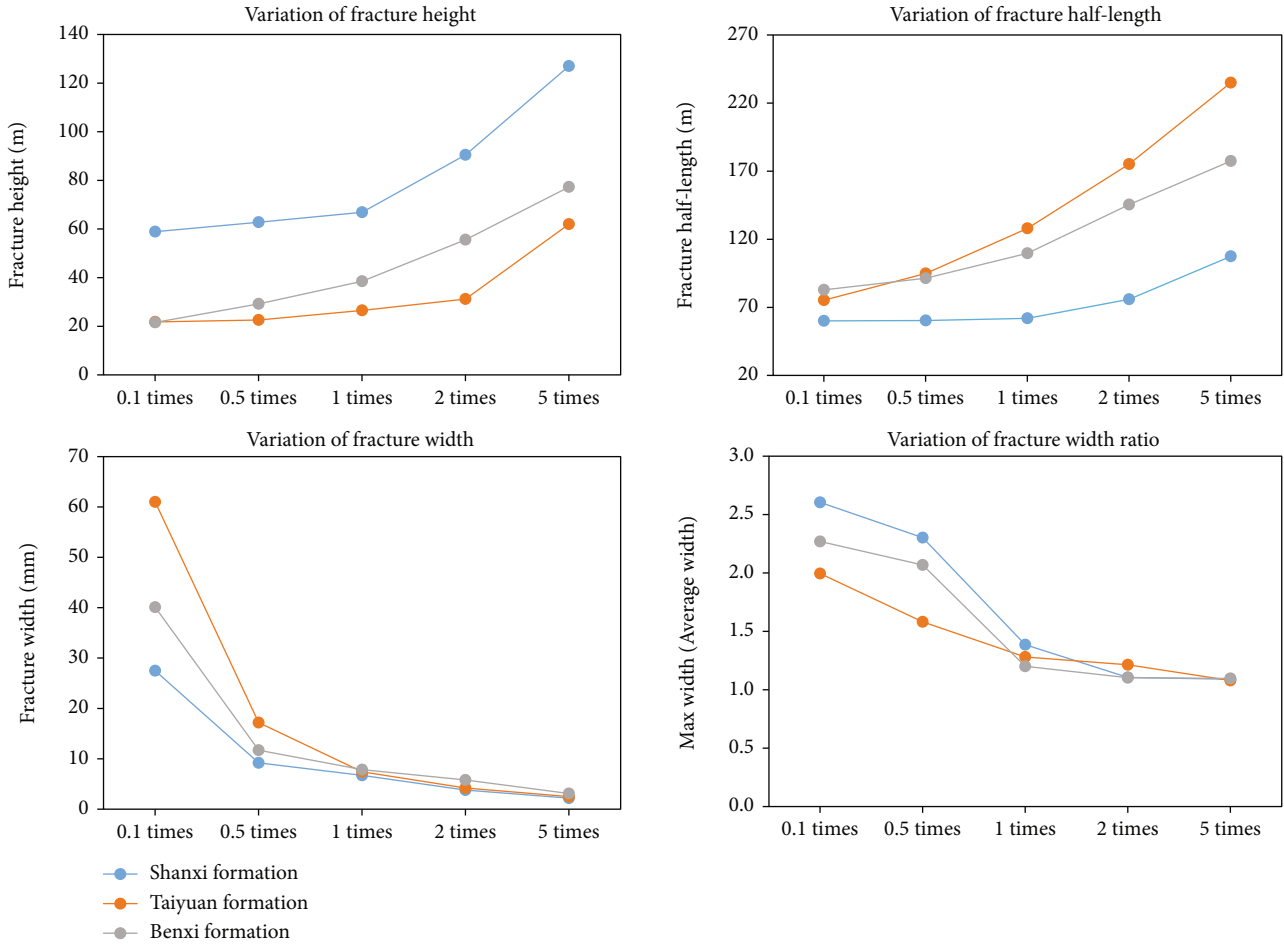
FIGURE 11: Variation of hydraulic fracture shape with the fracturing fluid injection rate.

break through the mudstone interlayers and leads to a large fracture height; since the total fracturing fluid volume is fixed and a large amount of it is consumed to generate the large fracture height, the amount of fracturing fluid used to generate the fracture half-length is small, so the fracture half-length is short. The hydraulic fracture of the Taiyuan formation is the best because the lower interlayer of the formation is the coal seam, which is thick and has a high geostress and creates a strong barrier effect to prevent the fracture from penetrating, so all of the fracturing fluid is used to generate fracture half-length within the sandstone layer. The hydraulic fracture of the Benxi formation shows the medium state because the upper and lower barriers are mudstone-coal intervals, and the barrier effect of which is weaker than that of pure coal but better than pure mudstone.

4. The Sensitivity Analysis of the Geological and Fracturing Operational Parameters

Based on the hydraulic fracturing numerical model constructed in Section 3 and the major influencing factors selected in Section 2.3, the sensitivity of the geological and fracturing operational parameters' effect on the hydraulic fracture propagation is simulated and analyzed.

4.1. The Sensitivity Analysis of Reservoir Geological Parameters

4.1.1. The Sensitivity Analysis of the Geostress Difference. According to the variation of geostress for different layers shown in Table 2, calculate the geostress difference variation range for these three formations. Simulate the fracture propagation under each geostress difference and record the variation of fracture height, half-length, and width along with the change of geostress differences, which is shown in Figure 6.

It can be seen from the figure that the geostress difference between the gas layer and interlayers shows a significant effect on fracture propagation. The fracture height decreases and the fracture half-length increases with the increase of the geostress difference, indicating that the increase of the geostress difference makes the fracture more difficult to break through the interlayer, which in turn promotes the lateral propagation of fractures within this formation. When the geostress difference increases to more than
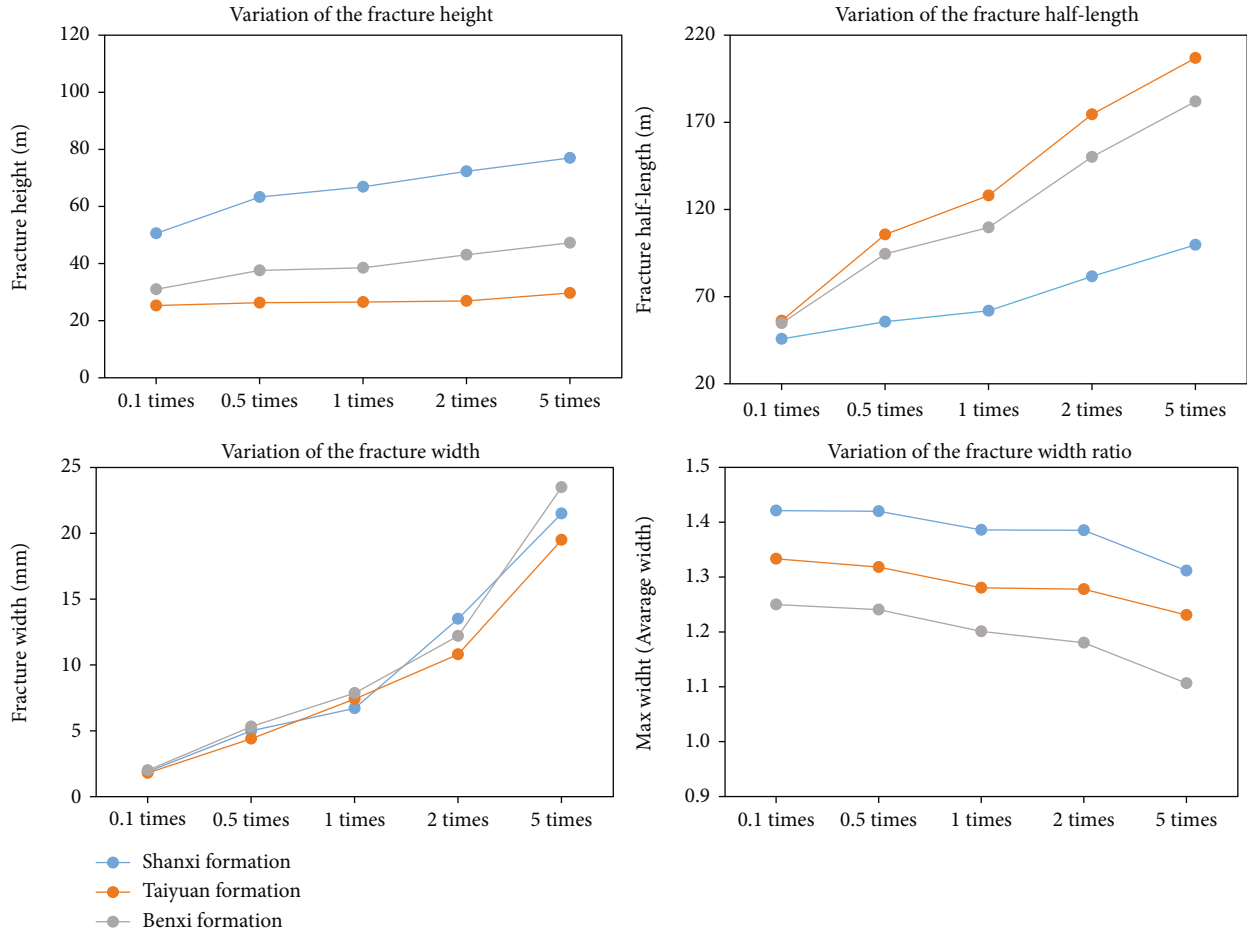
FIGURE 12: Variation of hydraulic fracture shape with the fracturing fluid injection volume.

8 MPa, the change of the fracture height and fracture length tends to stop, indicating that the fracture cannot penetrate the interlayers at all. The fracture widths do not change too much with the increase of the geostress difference, indicating that the effect of the geostress difference on the fracture width is limited.

4.1.2. The Sensitivity Analysis of the Elastic Modulus and Poisson's Ratio. Similar to the geostress, calculate the variation range of elastic modulus and Poisson's ratio between the gas layer and interlayers in Table 2. Simulate the fracture propagation under the different values of elastic modulus and Poisson's ratios, the results are compared in Figures 7 and 8. In these figures, the elastic modulus difference means the difference between the elastic modulus in the gas layer and the interlayers, as does the Poisson's ratio difference.

As can be seen, unlike the geostress difference, the difference of the elastic modulus and Poisson's ratio between the gas layer and interlayers has no obvious effect on the fracture propagation, and the fracture shape remains roughly unchanged.

4.1.3. The Sensitivity Analysis of the Layer Number. The sensitivity analysis of the layer number mainly focuses on the

Shanxi formation, since the geostructure of this formation is the overlapping of sandstone and mudstone. On the basis of not changing the overall thickness of the Shanxi formation, the gas layers are changed from 1 to 9 layers accordingly, and the influence of the geostress difference between the gas layer and interlayers is also considered, which varies from 1 to 6 MPa. Simulate the fracture propagation under the different layer numbers and geostress differences, the results are shown in Figure 9.

It can be seen from the figure that the fracture height first increases and then decreases with the increase of the layer number. When the number of layers is small, the interlayer is thicker, which inhibits the longitudinal propagation of the fracture; as the layer number increase, the thickness becomes thinner, so it is easier for fractures to break through the interlayer, and the fracture height increases. However, as the layer number continues increasing, the frequent changes in the geomechanical parameters between the gas layer and interlayer consume the energy of longitudinal propagation of the fracture, and then, the fracture height starts to decrease. The variation of the fracture width is similar to the fracture height, while the fracture half-length continues to decrease with the increasing number of layers. At the same time, under the same number of layers, the fracture height
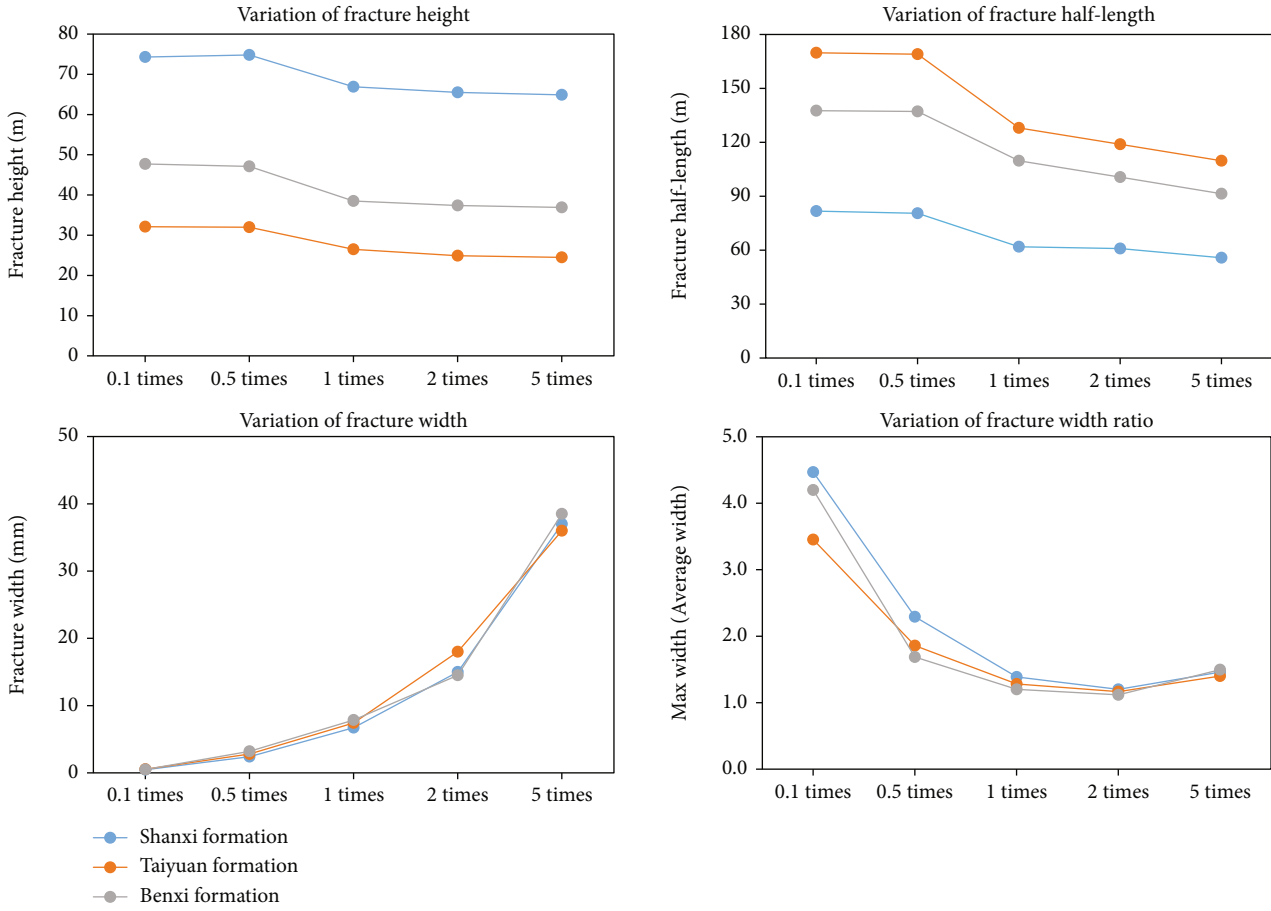
FIGURE 13: Variation of hydraulic fracture shape with the proppant density.

decreases with the increase of the geostress difference, while the fracture half-length and width increase, indicating that the increase of the geostress difference can still inhibit the longitudinal propagation and promote the horizontal propagation of the fracture, in the case of multilayer overlapping.

4.2. The Sensitivity Analysis of Fracturing Operational Parameters

4.2.1. The Sensitivity Analysis of the Fracturing Fluid Viscosity. In addition to geological parameters, fracturing operational parameters also have an important impact on fracture propagation. Fracturing fluid viscosity is the first parameter to be considered. In this paper, three different fracturing fluids which have different viscosities (shown in Figure 4), and the slickwater, the base fluid, and the gel are used for analysis. These three fracturing fluids are used as the prepad fluid+sand-carrying fluid, and the fractures under different fracturing fluids are shown in Figure 10.

As can be seen from the figure, as the viscosity of the fracturing fluid increases, the fracture height increases and the fracture half-length decreases, indicating that the increase in the fracturing fluid viscosity will promote the longitudinal propagation of the fracture and inhibit its lateral propaga-

tion. Among the three fracturing fluids, slickwater is the most favorable one for laterally creating fractures; meanwhile, the curves of fracture height and fracture half-length show obvious step-like changes. Under the same prepad fluid, the fracture height and fracture half-length are almost the same, indicating that fracture propagation mainly depends on prepad fluid; while the fracture width is mainly affected by the sand-carrying fluid, the higher the viscosity of the sand-carrying fluid is, the larger the fracture width will be. According to the ratio of the maximum fracture width to the average fracture width, the fracture width ratio under the slickwater is the largest, indicating that the fracture distribution is very uneven, mainly because the slickwater viscosity is too low, the sand-carrying capacity is weak, and the proppant settles seriously.

4.2.2. The Sensitivity Analysis of the Fracturing Fluid Injection Rate. Modify the fracturing fluid injection rate to 0.1 times, 0.5 times, 2 times, and 5 times of its original value (3.5 m³/min in Table 3) and simulate the fracture propagation under each injection rate, and the results are shown in Figure 11.

It can be seen from the figure that the fracture height and half-length all increase with the increase of injection
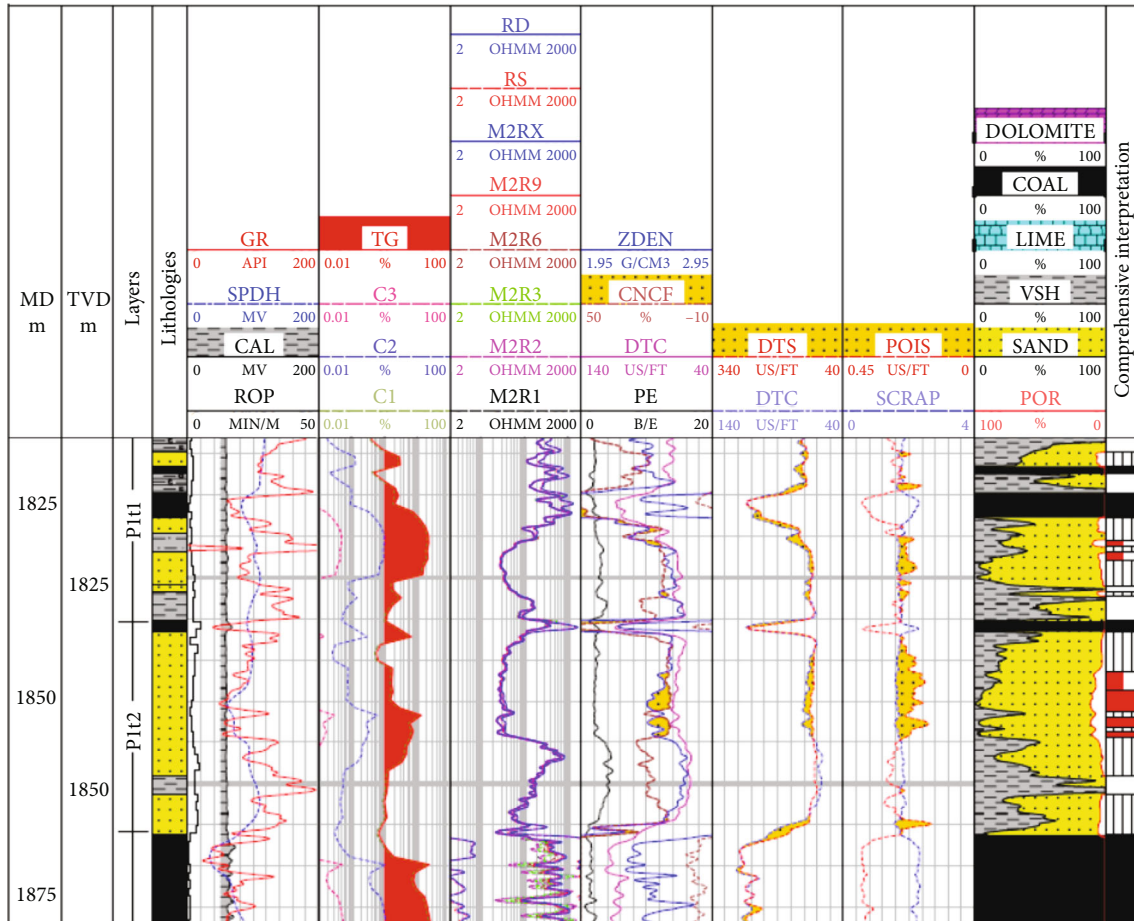
FIGURE 14: Well-logging curve in the Taiyuan formation of well X-1.

rate, indicating that the increase of injection rate will promote fracture propagation both in longitudinal and lateral directions, which is not a good choice for controlling fracture height in the multilayered reservoir. The fracture width decreases with the increase of the injection rate, but the fracture width and the fracture width ratio all present abnormally large values at the low injection rate, and this is mainly because the proppant cannot be carried to the deep fracture at the low injection rate and accumulates near the wellbore; when the injection rate is large, it is more powerful to bring the proppant into the deep fracture and makes an evenly distributed fracture width.

4.2.3. The Sensitivity Analysis of the Fracturing Fluid Injection Volume. Modify the fracturing fluid injection volume to 0.1 times, 0.5 times, 2 times, and 5 times of its original value (shown in the second column of Table 3) and simulate the fracture propagation under each injection volume, and the results are shown in Figure 12.

It can be seen from the figure that the fracture height and fracture half-length show a gentle increase trend with the increase of the injection volume, but the trend gradually slows down, which means that the method of expanding the fracture length by increasing the injection volume is uneconomical. Fracture width shows a dramatic increase

trend with injection volume since more injection volume brings more proppant which supports a larger fracture width.

4.2.4. The Sensitivity Analysis of the Proppant Concentration. Modify the proppant concentration in the fracturing fluid to 0.1 times, 0.5 times, 2 times, and 5 times of its original value (shown in the fourth column of Table 3) and simulate the fracture propagation under each proppant concentration, and the results are shown in Figure 13.

It can be seen from the figure that the fracture height and half-length slowly decrease with the increase of proppant concentration, while the fracture width increases significantly. The results indicate that proppant concentration has an inhibitory effect on fracture propagation, and the main function of proppant in the fracturing operation is to increase the fracture width. The fracture width ratio decreases with the increase of proppant concentration, indicating that with the increase of proppant concentration, and the fracture width becomes more regular; however, when the proppant concentration reaches 5 times the original value, the fracture width ratio increases. The reason may be that the proppant concentration is too large at this time, and the sand-carrying fluid can no longer effectively suspend this amount of proppant, resulting in the settlement of the proppant.

TABLE 4: Lithologies and geological parameters of different layers in Taiyuan formation of well X-1.

Lithology	Top depth (m)	Bottom depth (m)	Thickness (m)	Geostress (MPa)	Elastic modulus (10^4 MPa)	Poisson's ratio	Sg (%)	Poro (%)	Perm (mD)
Mudstone	1801.7	1809.9	8.2	30.2	3.32	0.30	0	0.69	0.01
Dry sandstone	1809.9	1811.5	1.6	28.4	3.65	0.26	0	6.27	0.19
Coal	1811.5	1812.5	1	28.1	3.21	0.26	0	1.75	0.04
Mudstone	1812.5	1814.8	2.3	27.6	3.35	0.24	0	0.06	0
Coal	1814.8	1817.8	3	34.7	0.77	0.36	0	0.73	0.01
Dry sandstone	1817.8	1820.6	2.8	29.4	2.40	0.28	0	4.85	0.08
Poor gas sandstone	1820.6	1823	2.4	27	4.25	0.23	17.02	4.63	0.08
Dry sandstone	1823	1826.1	3.1	26.9	4.86	0.23	2.28	3.22	0.05
Mudstone	1826.1	1830.3	4.2	28.1	4.66	0.26	0	1.75	0.02
Coal	1830.3	1831.6	1.3	32.8	0.88	0.33	0	0.12	0
Dry sandstone	1831.6	1836.5	4.9	27.3	4.93	0.23	0.81	2.82	0.04
Rich gas sandstone	1836.5	1841.3	4.8	25.5	4.55	0.20	48.92	9.04	1.26
Dry sandstone	1841.3	1842	0.7	27.2	4.52	0.23	0	8.58	0.50
Rich gas sandstone	1842	1843.4	1.4	25	4.48	0.18	28.51	9.66	1.13
Dry sandstone	1843.4	1849.2	5.8	29.2	5.62	0.27	8.14	4.34	0.16
Mudstone	1849.2	1851.5	2.3	29.7	6.09	0.27	0	0.82	0.01
Dry sandstone	1851.5	1854.2	4.8	28.55	3.90	0.25	0	4.16	0.10
Coal	1856.3	1859.1	12.2	36.3	0.61	0.37	0	0.14	0
Mudstone	1868.5	1871.1	2.6	34.2	2.53	0.34	0	0.01	0
Coal	1871.1	1872	0.9	33.1	1.38	0.33	0	0.01	0

TABLE 5: The injection pumping procedure for hydraulic fracturing of well X-1.

Fracturing injection stage	Injection volume (m^3)	Proppant concentration (kg/m^3)	Injection rate (m^3/min)	Single-stage injection time (min)	Total injection time (min)	Fluid type	Proppant type
1	50	0	5	10.0	10.0	Gel	/
2	20.5	73	5	4.1	14.1	Gel	40/70 mesh
3	50	0	5	10.0	24.1	Gel	/
4	31.6	145	5	6.3	30.4	Gel	30/50 mesh
5	37.8	218	5	7.6	38.0	Gel	30/50 mesh
6	45.3	290	5	9.1	47.0	Gel	30/50 mesh
7	45.3	363	5	9.1	56.1	Gel	30/50 mesh
8	34.8	435	5	7.0	63.1	Gel	30/50 mesh
9	11.9	508	5	2.4	65.4	Gel	30/50 mesh
10	19.1	0	5	3.8	69.3	Gel	30/50 mesh

5. Example: The Fracturing Simulation and Optimization of a Low Production Well in the Multilayered Thin Tight Sandstone Gas Reservoir

In this section, a real well X-1 in the multilayered thin tight sandstone gas reservoir in the Ordos Basin is selected as an example, and the well is a low-production well after hydraulic fracturing. We construct the geological model of this well and perform the hydraulic fracturing simulation according to field parameters, then analyze the reasons for its low production and propose an optimized hydraulic fracturing plan.

5.1. The Geological Condition and Hydraulic Fracturing Simulation of Well X-1. The well X-1 perforated and fractured the gas layer in the Taiyuan formation, but has a
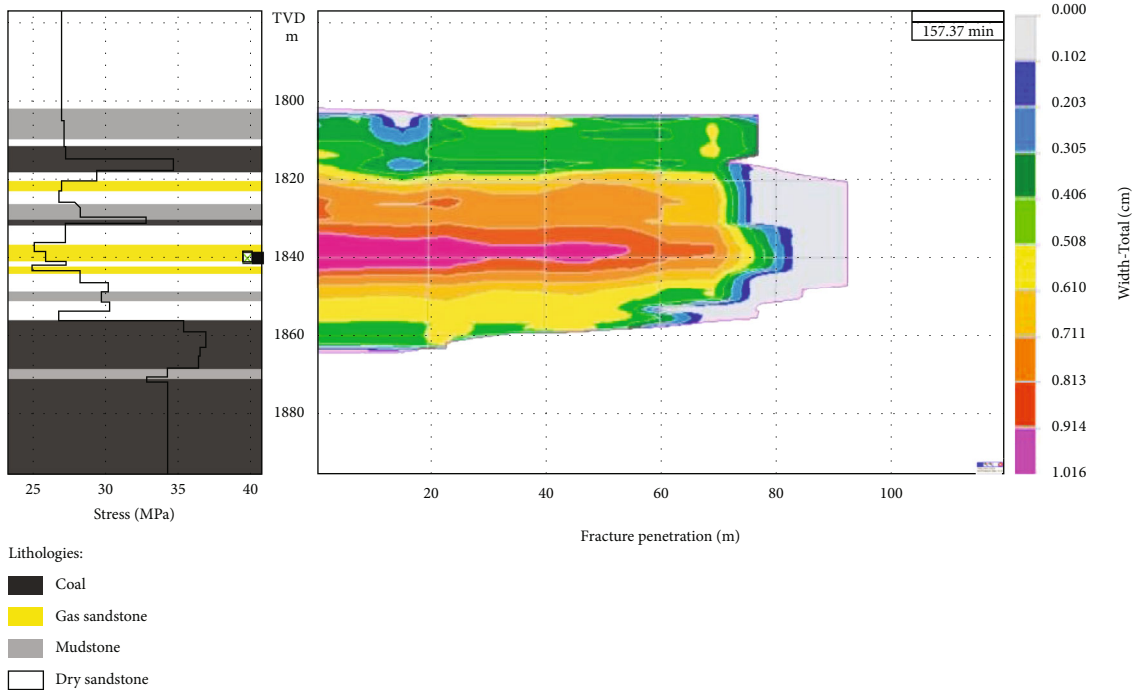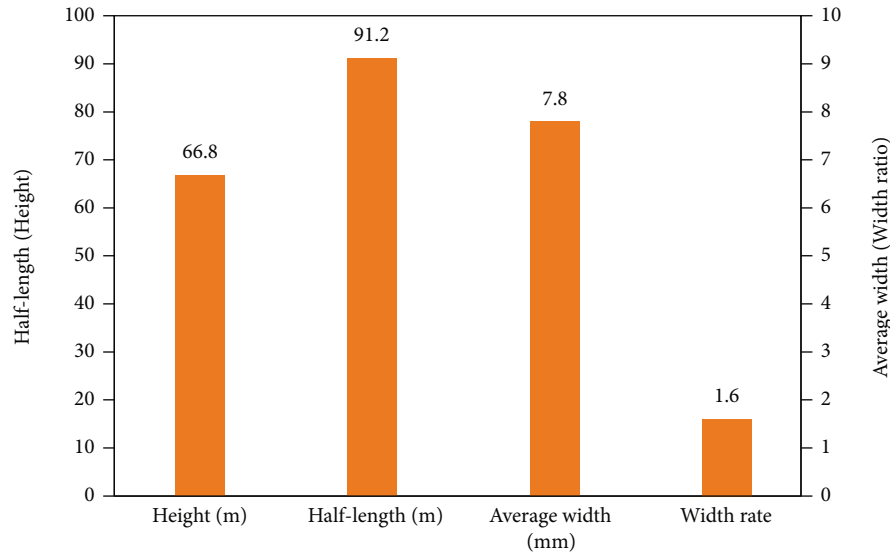
(a) The fracture distribution after simulation
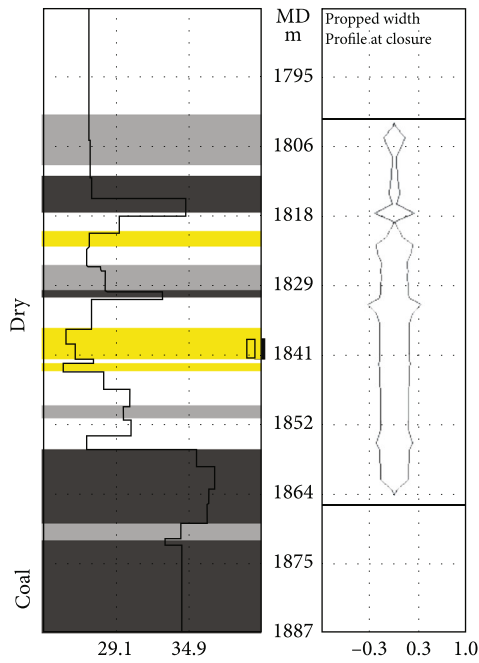
(b) The cross-section of the fracture

Figure 15: Continued.

(c) The values of fracture parameters

FIGURE 15: Distribution of the hydraulic fracture in the Taiyuan formation of well X-1.

problem of low production after fracturing. The open-flow gas rate after fracturing is only 3000 m³/d, which is far lower than the estimated value of 20000 m³/d. The logging curve of this well is shown in Figure 14, and the lithologies and geological parameters for every layer obtained from the well-logging interpretation are shown in Table 4.

From the well-logging curves and the lithology table, it can be seen that the upper part of the Taiyuan formation is a stratum of overlapped mudstone, dry sandstone, and coal seam, while the lower part of it is a thick coal seam. Between them is a total thickness of 8.7 m of good and poor gas layers, which are roughly divided into two parts by a thin coal seam in the middle as an interlayer. The rich gas layer is located in the lower part, which is the main gas production layer, and the poor gas layer is located in the upper part, with high water saturation and little production potential.

Then, perform the hydraulic fracturing simulation. The fracturing fluid used is the CPF-WBFF-FW fracturing fluid system, which consisted of a low-viscosity base fluid and a high-viscosity gel, relevant rheological parameters are shown in Figure 4 of Section 3.3. The proppant is 40/70 mesh and 30/50 mesh ceramic proppant, the vertical depth of the perforation interval is 1849.0 m-1852.5 m, and the perforation density is 16 holes/m, with the hole diameter of 10.6 mm. The fracturing pump injection parameters used for this well are shown in Table 5.
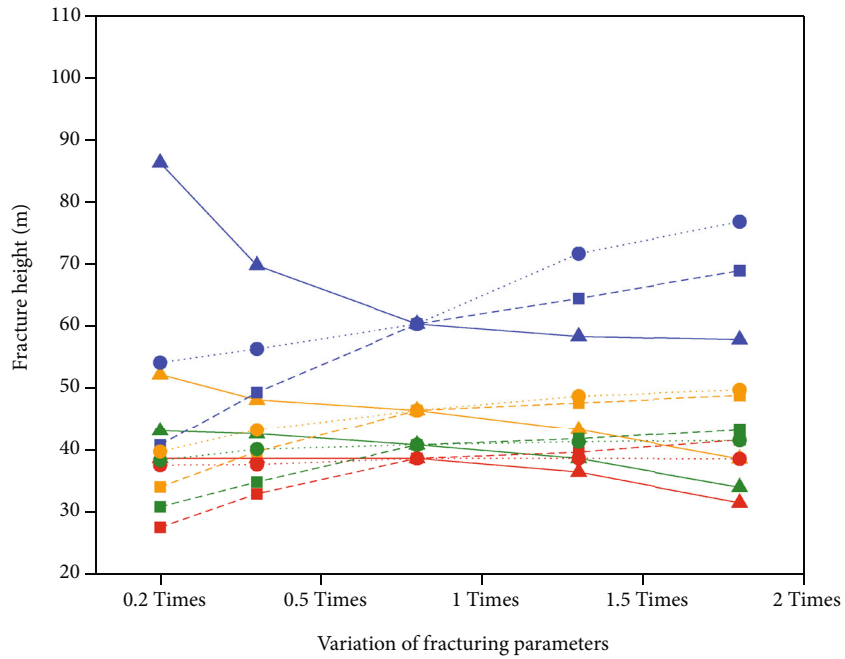
According to the lithology and geological parameters shown in Table 4, the numerical model of the multilayered thin tight sandstone gas reservoir is established by using StimPlan software; then, according to the fracturing pump injection parameters shown in Table 5, the hydraulic fracturing simulation is performed, and the fracture of well X-1 is shown in Figure 15.

It can be seen from the simulation results that the fracture height is too large, reaching 63 m, which is more than 10 times of the effective rich gas layer's thickness, breaking

through the coal seam, mudstone layer, and the poor gas layer, and these layers have relatively high water content; meanwhile, the fracture half-length is only 90 meters, which cannot laterally propagate deep into the rich gas layer. The main reason for such a fracture shape is that the fracturing injection procedure is unreasonable. From Table 5, it can be seen that the fracture prepad fluid and sand-carrying fluid are all consisted of gel, summarizing from Section 4.2.1, such a high-viscosity fracturing fluid will promote the longitudinal propagation of the fracture and inhibit its lateral propagation, making it easy for fractures to break the interlayer, resulting in a too large fracture height and too short fracture half-length; in addition, the proppant concentration and distribution in the fracture are also low and settles, resulting in a narrow and uneven cross-section, indicating that the fracture conductivity is poor. According to the simulation results, it is speculated that the integration of these factors causes the low production of this well.

5.2. The Hydraulic Fracturing Sensitivity Analysis and Hydraulic Fracturing Scheme Optimization of Well X-1. According to the analysis results that the fracture height is too large and the fracture half-length is insufficient due to the original fracturing scheme, the hydraulic fracturing optimization design is carried out, in order to construct a fracture with a lower height, longer half-length, wider and more even width, and better conductivity. First, based on the reservoir's geological condition, the sensitivity analysis of fracture parameters is carried out. Add the low-viscosity slickwater to the fracturing fluid system and design and compare four fracturing fluid systems based on the prepad fluid+sand-carrying fluid type: the slickwater+base fluid system, the base fluid+gel system, the slickwater+gel system, and the gel+gel system. At the same time, analyze the influence of the injection rate, the injection volume, and the proppant concentration, and the above parameters are
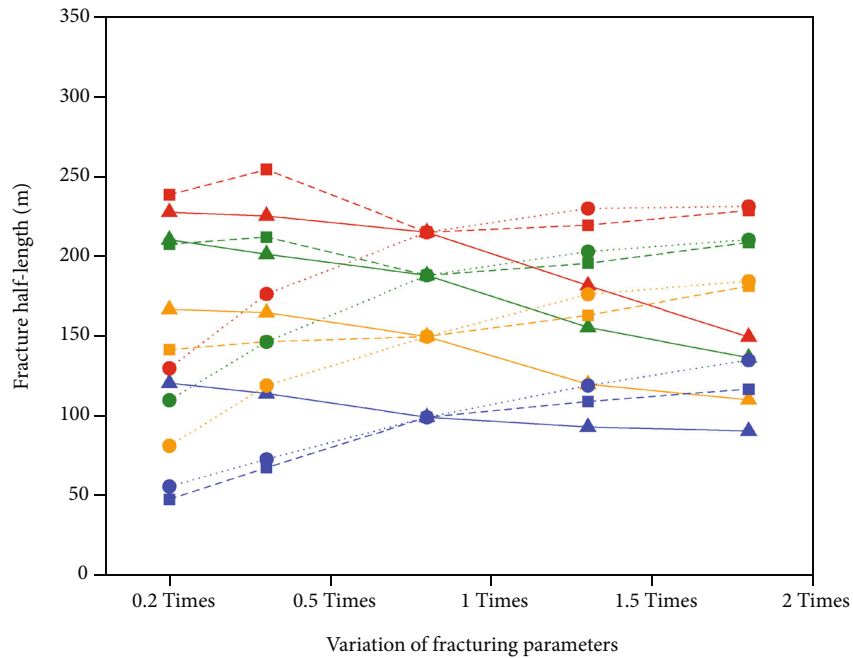
(a) Variation of the fracture height under different fracturing parameters

(b) Variation of the fracture half-length under different fracturing parameters
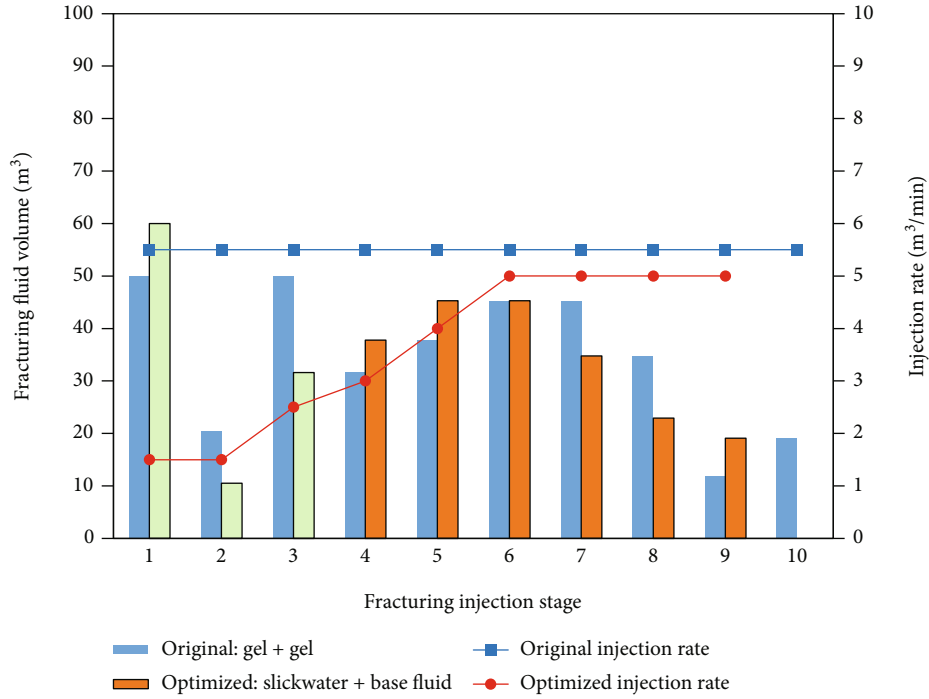
Figure 16: Continued.
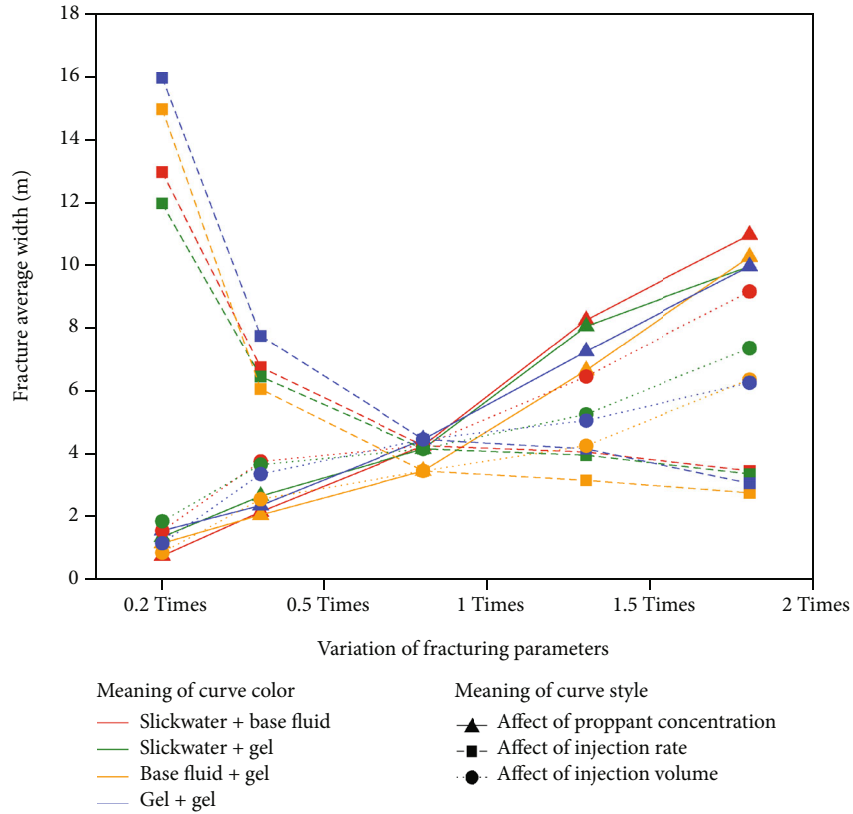
(c) Variation of the fracture average width under different fracturing parameters
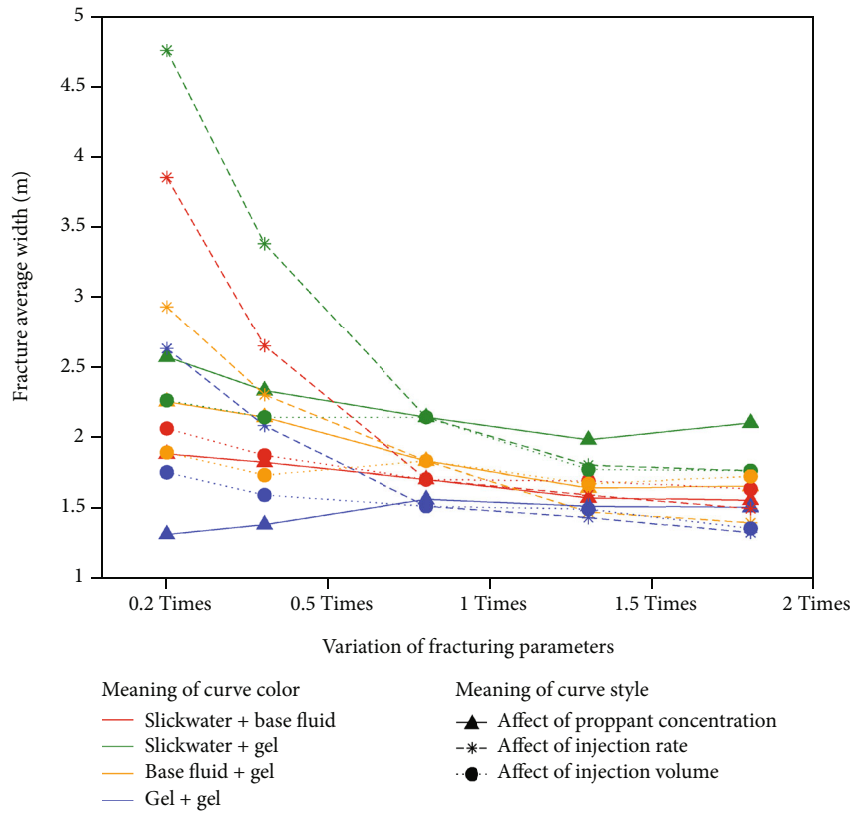
(d) Variation of the fracture width ratio under different fracturing parameters

FIGURE 16: Sensitivity analysis of the fracture parameters.

(a) The comparison of fracturing fluid, injection volume, and injection rate at every fracturing injection stage before and after optimization
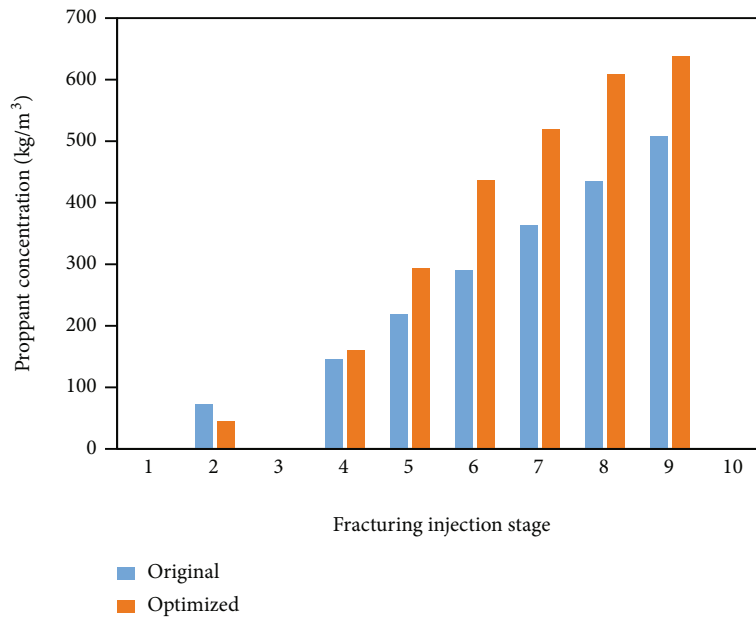
(b) The comparison of proppant concentration at every fracturing injection stage before and after optimization

FIGURE 17: Comparison of original and optimized hydraulic fracturing schemes.

adjusted to 0.2 times, 0.5 times, 1.5 times, and 2 times of the original value. Then, perform the fracturing simulation and record the variation of fracture parameters, and the results are shown in Figure 16.

As shown in the figure, the influence of various parameters on fracture propagation can be seen. First, for fracturing fluid, the combination of low and high-viscosity fracturing fluids has a better effect than simply using the gel. Among them, the use of slickwater as the prepad fluid can signifi-

cantly increase the fracture half-length and control the fracture height, the same as the conclusion of Section 4.2.1; additionally, the fracturing effect of the fracturing fluid system slickwater+base fluid is better than that of the slickwater+gel. Second, for the injection rate, the fracture half-length under the fracturing fluid of slickwater is better when injected at a low rate, while the fracture half-length under the fracturing fluid of base fluid or gel is better when injected at a high rate. However, when slickwater is injected at a low
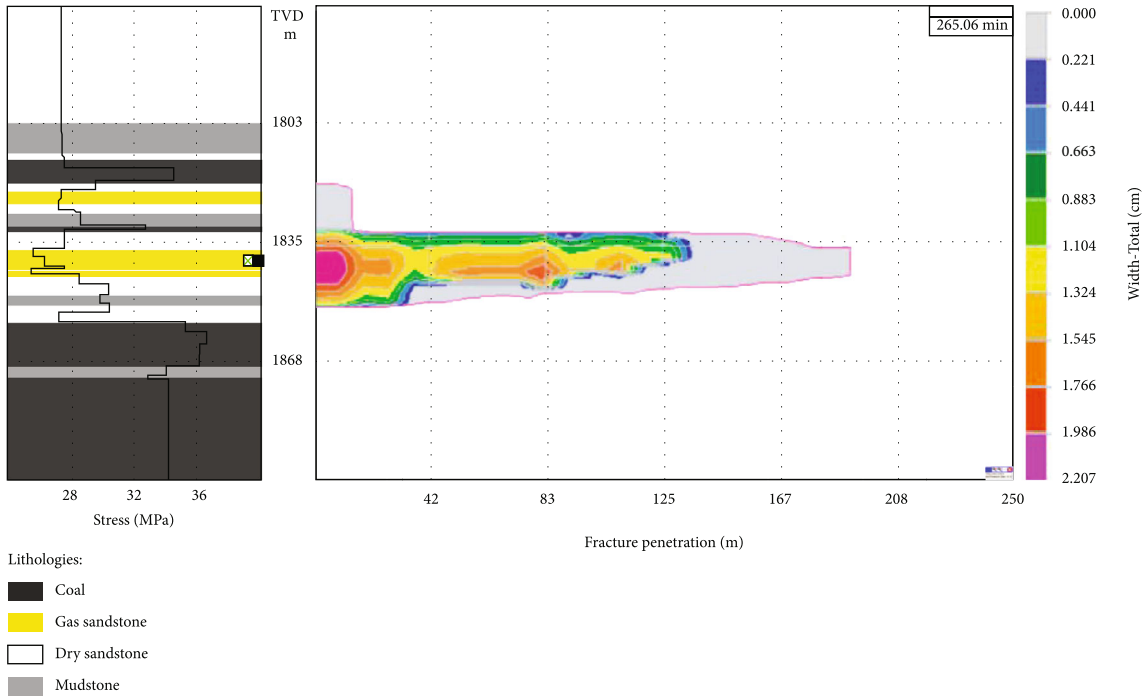
Figure 18: The optimized hydraulic fracture for well X-1.
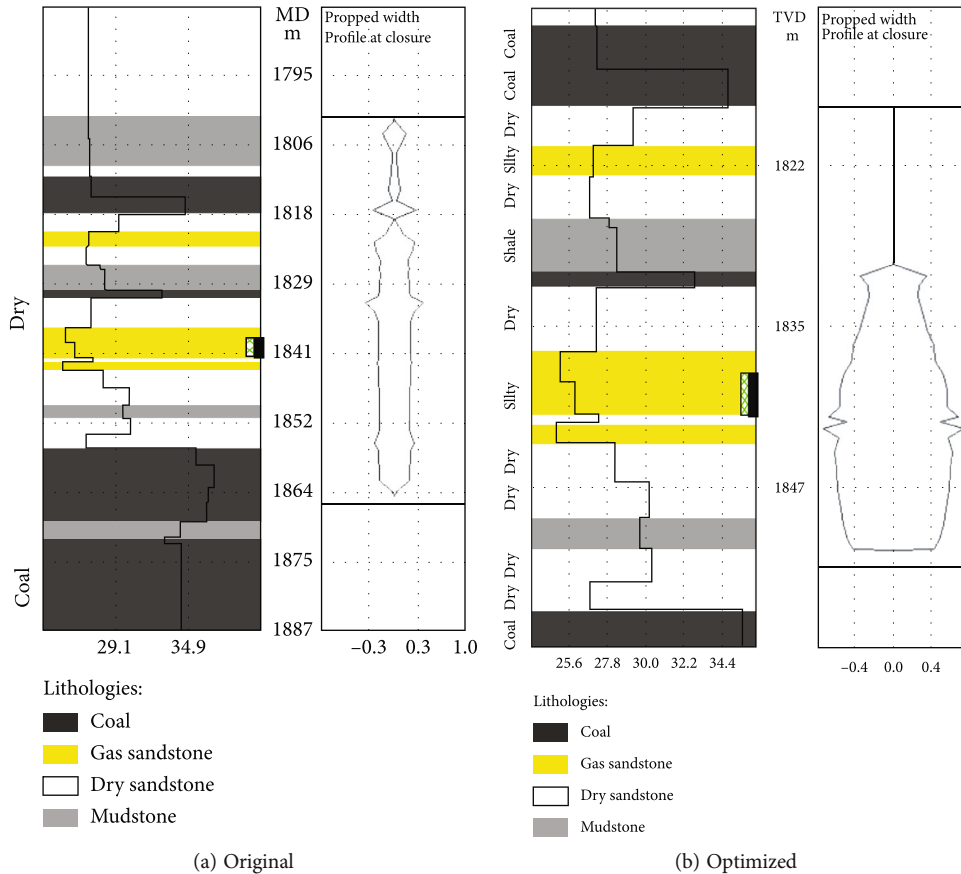

(a) Original

(b) Optimized

Figure 19: The comparison of original and optimized fracture cross-sections.
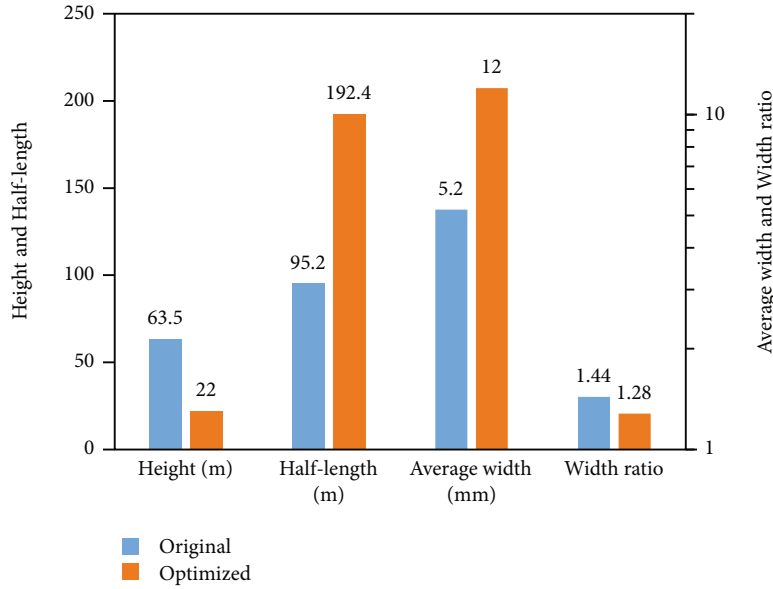
FIGURE 20: The comparison of original and optimized fracture parameters.

TABLE 6: Reservoir and fracture production simulation parameters of well X-1.

Reservoir properties	
Area (km^2)	0.5
Formation initial pressure (MPa)	18.4
Formation temperature (˚C)	52
Tubing ID (cm)	4.06
Gas relative density	0.69
Gas viscosity (cp)	0.019
Gas compressibility (10^{-6} 1/MPa)	52475
Z factor	0.848
CH$_4$ percentage (%)	90.8
Original fracture properties	
Half-length (m)	95
Height (m)	63
Width (mm)	5.6
Conductivity (D-cm)	12
Optimized fracture properties	
Half-length (m)	192
Height (m)	22
Width (mm)	11.9
Conductivity (D-cm)	54

rate, the proppant settles seriously. Third, for the injection volume, the half-length and height of the fracture increase while increasing the injection volume, but the magnitude is not obvious, and the injection volume is directly related to the fracturing cost, so it is not economical to optimize the fracture propagation by increasing the injection volume.

Finally, for the proppant concentration, after increasing the proppant concentration, both the fracture height and half-length decrease, while the fracture width increases significantly. Therefore, the proppant concentration should be reduced in the prepad fluid and can be increased in the sand-carrying fluid.

Based on the above analysis, fracturing in the multilayered thin tight gas reservoir is not suitable for using high-viscosity fracturing fluid, so the optimized hydraulic fracturing schemes adopt a slickwater+base fluid system, in which slickwater is injected as prepad fluid at a low rate (1-3 m^3/min), and the base fluid is injected as the sand-carrying fluid at a high rate (3-6 m^3/min), the proppant concentration in the prepad fluid is adjusted to 70-100% of the original value and is adjusted to 100-130% of the original value in the sand-carrying fluid, and the injection volume is not adjusted in a large range. Within this range, a fine adjustment is made based on simulation, and the final optimized hydraulic fracturing scheme is shown and compared with the original one in Figure 17.

The hydraulic fracture generated by the optimized fracturing scheme is shown from Figures 18–20. Comparing it with the original fracture, it can be seen that the fracture half-length increases from 95 m to 192 m, extending deeper into the rich gas layer; at the same time, the fracture height decreases from 63 m to 35 m, most of which do not break through the thin interlayer, and the effective fracture height is only 22 m. It is proved that the method of injecting slickwater at a low rate can effectively control the fracture height in the thin tight gas reservoir with weak interlayers. Furthermore, from the cross-section comparison, it can be seen that the average width of the fracture increases from 5.2 mm to 12 mm, the proppant is more evenly distributed in the fracture, and the conductivity of the fracture is significantly improved.
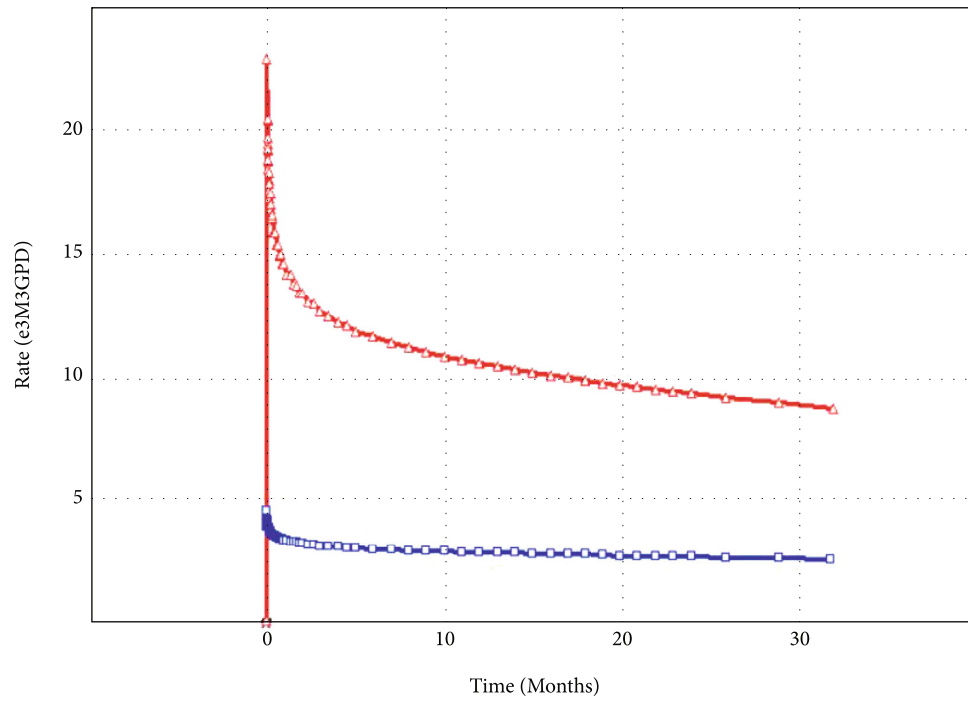
(a) The comparison of instantaneous gas production rate
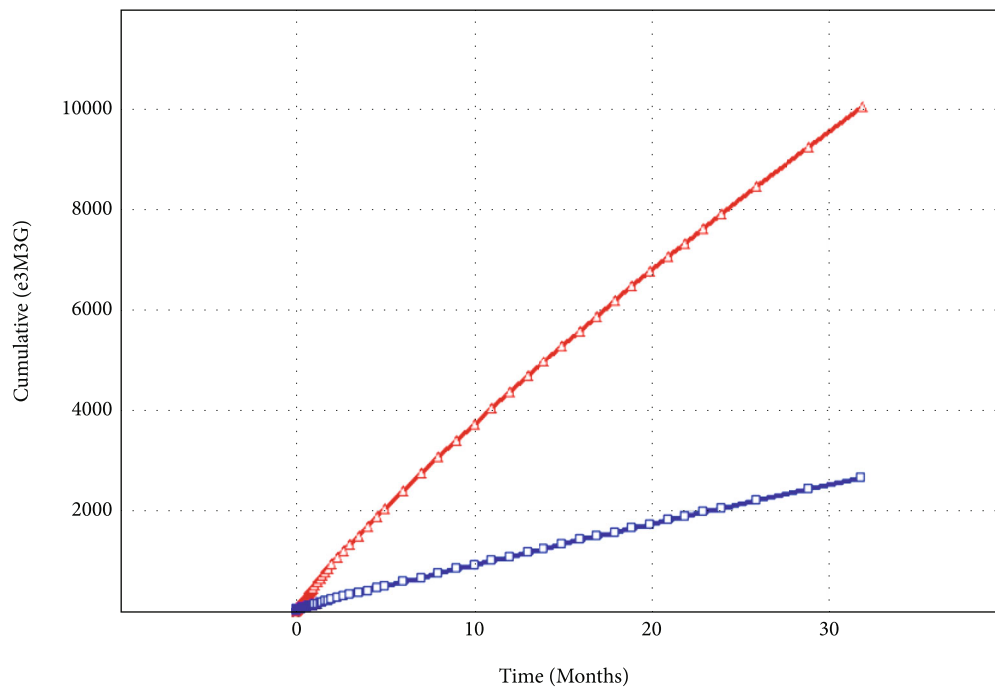
(b) The comparison of cumulative gas production

FIGURE 21: The comparison of gas production for the original and optimized hydraulic fractures.

TABLE 7: Hydraulic fracture parameters for wells A and B in the Daniudi gas reservoir [23].

Fracture parameters	Fracture length (m)	Fracture height (m)	Fracture width (cm)	Fracture conductivity (D.cm)	Open-flow gas rate ($10^4 \, \text{m}^3$/d)
Well A	214	25	0.3	21.3	10.8
Well B	201	33	0.4	20.4	5.2

5.3. The Productivity Comparison of the Original and Optimal Fractures of Well X-1. The production capacities of the original and optimized fractures are compared, and the numerical reservoir model module in the StimPlan software is used to simulate the production of tight gas. The relative parameters of the tight gas reservoir and the original and optimized fractures are shown in Tables 4 and 6. The production simulation time is 3 years, the wellhead pressure is fixed at 5.5 MPa. The instantaneous gas production rate and cumulative gas production of the original and optimal fractures are shown in Figures 20 and 21, respectively, where the blue curves represent the original fracture, the red curves represent the optimized fracture, and the unit e3M3G stands for thousand cubic meters of gas, and e3M3GPD stands for thousand cubic meters of gas per day.

It can be seen from the figure that the optimized fracture productivity is obviously better than that of the original one. Since the fracture height is effectively controlled, the connection to the high water-bearing layers is avoided, and the fracture half-length extends longer into the rich gas layer, which made the instantaneous gas production rate increase to three times that of the original fracture; besides, the cumulative gas production in three years is far more than 2.5 e3M3G of the original fracture, reaching more than 10 e3M3G. The comparison of fracture shape and productivity before and after optimization shows that the optimized fracture is better than the original fracture in many aspects.

The well X-1 is a pretty new well that just developed in these recent years, and the optimized fracturing scheme has not been applied to this well practically; however, a practical hydraulic fracturing example for wells in the Daniudi gas reservoir can help prove the reliability of the optimized hydraulic fracturing scheme proposed in this paper. The Daniudi gas reservoir is also located in the Ordos Basin and also has thin and multilayered tight sandstone gas formations with weak mudstone interlayers. The depth of the main gas layer is 2600 m with an average thickness of 10 m, the average porosity is 9.3%, and the average permeability is 0.76 mD. The geostress difference between the gas layer and interlayers is 2.8 MPa. According to this geological condition, two adjacent wells in this reservoir that perforated in the same gas layers were compared by using different hydraulic fracturing schemes. Well A was fractured using a hydraulic fracturing scheme that was similar to the optimized hydraulic fracturing scheme proposed in this paper: first is the low viscosity fracturing fluid (10 mPa.s) at a low injection rate (3 m³/s), followed by medium viscosity fracturing fluid (40 mPa.s) at a medium injection rate (3.5 m³/s), and the last is high-viscosity fracturing fluid (80 mPa.s) at a high injection rate (4 m³/s). As a comparison, Well B was fractured using traditional high-viscosity fracturing fluid (80 mPa.s) at a constant injection rate (4.5 m³/s). The total fluid volumes injected for these two well were almost the same [23]. After observation, the hydraulic fracture parameters for wells A and B are shown in Table 7.

As shown in Table 7, compared with well B, well A has a longer fracture length, and the fracture height is better controlled; with better fracture shape and higher fracture conductivity, the open-flow gas rate for well A is nearly twice as that of well B, which is fractured using the traditional methods. Summing up this practical fracturing example, we can see that facing the similar thin and multilayered formations, the technicians for the Daniudi gas reservoir chose a similar fracturing scheme as proposed in this paper and obtained significant fracturing and production results. This practical fracturing example helps prove the reliability of this research, that the optimized hydraulic fracturing scheme can improve the development of multilayered thin tight sandstone gas reservoirs.

6. Conclusions

In this paper, the numerical simulation method is used to study the hydraulic fracture propagation mechanism in the multilayered thin tight sandstone gas reservoir based on a real reservoir in the Ordos Basin. The sensitivity analysis of different geological and fracturing operation parameters is performed, based on which, a real low-production well after fracturing in this kind of reservoir is analyzed, and an optimized hydraulic fracturing scheme for this well is proposed. The conclusions of this paper are summarized as follows:

(1) The vertical structure of the multilayered thin tight sandstone gas reservoir is different from the traditional gas reservoir, and the gas layers are usually thinner than 10 m and intersected with water-bearing layers; the interlayers are also thin and weak, which are easy to be penetrated by hydraulic fractures under improper fracturing schemes, causing wellbore water flooding and low gas production

(2) For the reservoir geological parameters, the geostress shows a great impact on the fracture propagation, while the impacts of the elastic modulus and Poisson's ratio are not obvious. For the fracturing operational parameters, the low-viscosity fracturing fluid is good for controlling the fracture height, but not good for the proppant carrying, while the high-viscosity fracturing fluid is just the opposite. A high injection rate is not good for fracture control under thin interlayers, while a high proppant concentration

will prohibit fracture propagation and help control the fracture height

(3) Fracture propagation mainly occurs in the prepad fluid injection stage, while the sand-carrying fluid mainly affects the fracture width and conductivity. Injecting slickwater at a low rate (1-2 m^3/min) and keeping a low proppant concentration (lower than 80 kg/m^3) will help prevent fractures from breaking through thin interlayers and make better horizontal propagation. Then, injecting high-viscosity fracturing fluids at a medium rate (4-5 m^3/min) with a high proppant concentration (500-600 kg/m^3) can help control fracture height and ensure a large and evenly distributed fracture width and a better fracture conductivity

Data Availability

Data are available on request.

Conflicts of Interest

The authors declare that they have no conflicts of interest.

References

[1] C. Zou, Q. Zhao, J. Chen et al., "Natural gas in China: development trend and strategic forecast," *Natural Gas Industry B*, vol. 5, no. 4, pp. 380–390, 2018.

[2] M. Xinhua, J. Ailin, T. Jian, and H. Dongbo, "Tight sand gas development technology and practices in China," *Petroleum Exploration and Development*, vol. 39, no. 5, pp. 611–618, 2012.

[3] J. Yao, Z. X. Sun, K. Zhang, Q. Zeng, X. Yan, and M. Zhang, "Scientific engineering problems and development trends in unconventional oil and gas reservoirs," *Petroleum Science Bulletin*, vol. 1, no. 1, pp. 128–142, 2016.

[4] S. A. Khristianovic and Y. P. Zheltov, "Formation of vertical fractures by means of highly viscous liquid," in *4th World Petroleum Congress*, OnePetro, 1955.

[5] T. K. Perkins and L. R. Kern, "Widths of hydraulic fractures," *Journal of Petroleum Technology*, vol. 13, no. 9, pp. 937–949, 1961.

[6] K. Wu, *Numerical Modeling of Complex Hydraulic Fracture Development in Unconventional Reservoirs*, The University of Texas at Austin, 2014.

[7] R. Lin, L. Ren, J. Zhao, L. Wu, and Y. Li, "Cluster spacing optimization of multi-stage fracturing in horizontal shale gas wells based on stimulated reservoir volume evaluation," *Arabian Journal of Geosciences*, vol. 10, no. 2, pp. 1–15, 2017.

[8] E. Gordeliy and A. Peirce, "Coupling schemes for modeling hydraulic fracture propagation using the XFEM," *Computer Methods in Applied Mechanics and Engineering*, vol. 253, pp. 305–322, 2013.

[9] X. Garcia, N. Nagel, F. Zhang, M. Sanchez-Nagel, and B. Lee, "Revisiting vertical hydraulic fracture propagation through layered formations–a numerical evaluation," in *47th US Rock Mechanics/Geomechanics Symposium*, San Francisco, California, 2013.

[10] H. Zhang and J. J. Sheng, "Numerical simulation and optimization study of the complex fracture network in naturally fractured reservoirs," *Journal of Petroleum Science and Engineering*, vol. 195, article 107726, 2020.

[11] R. Zhang, G. S. Li, and J. C. Guo, "Experimental research into fracture propagation of complex lithologies in fractured tight oil reservoirs," *Petroleum Science Bulletin*, vol. 1, no. 3, pp. 353–362, 2016.

[12] M. J. Mayerhofer, E. P. Lolon, N. R. Warpinski, C. L. L. Cipolla, D. Walser, and C. M. M. Rightmire, "What is stimulated reservoir volume?," *SPE Production & Operations*, vol. 25, no. 1, pp. 89–98, 2010.

[13] X. Weng, O. Kresse, D. Chuprakov, C. E. Cohen, R. Prioul, and U. Ganguly, "Applying complex fracture model and integrated workflow in unconventional reservoirs," *Journal of Petroleum Science and Engineering*, vol. 124, pp. 468–483, 2014.

[14] X. Du, L. Cheng, J. Chen, J. Cai, L. Niu, and R. Cao, "Numerical investigation for three-dimensional multiscale fracture networks based on a coupled hybrid model," *Energies*, vol. 14, no. 19, p. 6354, 2021.

[15] I. D. Palmer and H. R. Craig, "Modeling of asymmetric vertical growth in elongated hydraulic fractures and application to first MWX stimulation," in *SPE Unconventional Gas Recovery Symposium*, Pittsburgh, Pennsylvania, 1984.

[16] R. J. Clifton and A. S. Abou-Sayed, "On the computation of the three-dimensional geometry of hydraulic fractures," in *Symposium on low permeability gas reservoirs*, Denver, Colorado, 1979.

[17] B. Chen, B. R. Barboza, Y. Sun et al., "A review of hydraulic fracturing simulation," *Archives of Computational Methods in Engineering*, vol. 29, pp. 1–58, 2021.

[18] M. P. Cleary, "Comprehensive design formulae for hydraulic fracturing," in *SPE annual technical conference and exhibition*, Dallas, Texas, 1980.

[19] E. Siebrits and A. P. Peirce, "An efficient multi-layer planar 3D fracture growth algorithm using a fixed mesh approach," *International Journal for Numerical Methods in Engineering*, vol. 53, no. 3, pp. 691–717, 2002.

[20] M. K. Rahman, M. M. Hossain, and S. S. Rahman, "An analytical method for mixed-mode propagation of pressurized fractures in remotely compressed rocks," *International Journal of Fracture*, vol. 103, no. 3, pp. 243–258, 2000.

[21] L. Vandamme and J. H. Curran, "A three-dimensional hydraulic fracturing simulator," *International Journal for Numerical Methods in Engineering*, vol. 28, no. 4, pp. 909–927, 1989.

[22] S. H. Advani, T. S. Lee, and J. K. Lee, "Three-dimensional modeling of hydraulic fractures in layered media: part I—finite element formulations," *Journal of Energy Resources Technology*, vol. 112, no. 1, pp. 1–9, 1990.

[23] W. Liu, "Application of "fracture network" fracturing technique in repeated fracturing wells in Daniudi gasfield," *Petrochemical Industry Application*, vol. 39, no. 3, pp. 9–13, 2020.